Journal of Cellular Physiology

Puromycin Insensitive Leucyl-Specific Aminopeptidase (PILSAP) Affects RhoA Activation in Endothelial Cells

TAKAHIRO SUZUKI,[1,2] MAYUMI ABE,[1] HIROKI MIYASHITA,[1] TOSHIMITSU KOBAYASHI,[2] AND YASUFUMI SATO[1]*

[1]*Department of Vascular Biology, Institute of Development, Aging and Cancer, Tohoku University, Sendai, Japan*

[2]*Department of Otolaryngology-Head and Neck Surgery, Tohoku University Graduate School of Medicine, Sendai, Japan*

Puromycin insensitive leucyl-specific aminopeptidase (PILSAP) expressed in endothelial cells (ECs) plays an important role in angiogenesis due to its involvement in migration, proliferation and network formation. Here we examined the biological function of PILSAP with respect to EC morphogenesis and the related intracellular signaling for this process. When mouse endothelial MSS31 cells were cultured, a dominant negative PILSAP mutant converted cell shape to disk-like morphology, blocked stress fiber formation, and augmented membrane ruffling in random directions. These phenotypic changes led us to test whether PILSAP affected activities of Rho family small G-proteins. Abrogation of PILSAP enzymatic activity or its expression attenuated RhoA but not Rac1 activation during cell adhesion. This attenuation of RhoA activation was also evident when G-protein coupled receptors such as proteinase-activated receptor or lysophosphatidic acid receptor were activated in ECs. These results indicate that PILSAP affects RhoA activation and that influences the proper function of ECs.

J. Cell. Physiol. 211: 708–715, 2007.

Angiogenesis is the formation of new blood vessels through endothelial cell (EC) proliferation and migration in combination with tubular morphogenesis. Angiogenesis is indispensable for various physiological and pathological processes, such as embryonic development, wound healing, diabetic retinopathy, and solid tumor growth. A number of molecules regulate angiogenesis both positively and negatively. However, the molecular mechanism of angiogenesis is not yet completely understood.

We searched for novel molecules involved in angiogenesis regulation, and isolated puromycin insensitive leucyl-specific aminopeptidase (PILSAP) with the use of subtraction strategy whose expression was augmented during the in vitro differentiation of murine embryonic stem (ES) cells to ECs (Miyashita et al., 2002). The expression of PILSAP in ECs is evident at the site of angiogenesis in vivo, and is regulated, at least in part, by a transcription factor polyomavirus enhancer-binding protein 2 (PEBP2) (Miyashita et al., 2002; Niizeki et al., 2004). Interestingly, endoplasmic reticulum aminopeptidase associated with antigen processing (ERAAP) was found to be identical to PILSAP, which was involved in the cleavage of various peptides for antigen presentation by MHC class I molecules (Serwold et al., 2002). Nevertheless, our analyses have revealed that PILSAP plays an important role in angiogenesis by its involvement in migration, proliferation and network formation (Akada et al., 2002; Miyashita et al., 2002). Aminopeptidases catalyze the sequential removal of amino acids from unblocked N-termini of peptides and proteins and play important roles in various biological processes, such as maturation, activation, modulation, degradation of bioactive peptides (Taylor, 1993). PILSAP belongs to the M1 aminopeptidase family, which contains an HEXXH(18X)E motif and a central Zn^{2+} ion essential for enzymatic activity. We examined the mechanism by which PILSAP regulates vascular endothelial growth factor (VEGF)-stimulated proliferation of ECs. As PILSAP is an aminopeptidase, PILSAP is expected to modulate cell function by catalyzing its physiological substrates. Our analysis have revealed that PILSAP binds to phosphatidylinositol-dependent kinase1 (PDK1) and removes 9 amino acids from the PDK1 N-terminus, which subsequently allows S6 kinase (S6K) to associate with PDK1 and PILSAP upon VEGF stimulation (Yamazaki et al., 2004).

Cell migration is a mechanically integrated molecular process that involves dynamic, coordinated changes in cell adhesions and cytoskeletal reorganization. The migration process includes protrusion of the leading edge, formation of new adhesions at the front, cell contraction, and the release of adhesions at the rear (Lauffenburger and Horwitz, 1996; Sheetz et al., 1998; Li et al., 2005). Reorganization of actin cytoskeleton generates locomotive force, and this process is regulated by Rho family small GTPases such as RhoA, Rac, and Cdc42. Rho family small GTPases act as molecular switches by cycling between GTP- and GDP-bound states and transmit extracellular chemotactic signals to downstream effectors. Activated Rac and Cdc42 induce reorganization of actin cytoskeleton at the leading edge. This reorganization of actin

Contract grant sponsor: Scientific Research on Priority Areas of the Japanese Ministry of Education, Science, Sports and Culture;
Contract grant number: 16022205.
Contract grant sponsor: Ministry of Education, Science, Sports and Culture of Japan;
Contract grant number: 17014006.

Mayumi Abe's present address is Department of Nanomedicine, Tokyo Medical and Dental University Graduate School, 1-5-45 Yushima, Bunkyo-ku, Tokyo 113-8519, Japan.

*Correspondence to: Yasufumi Sato, Department of Vascular Biology, Institute of Development, Aging and Cancer, Tohoku University, 4-1 Seiryo-machi, Aoba-ku, Sendai 980-8575, Japan.
E-mail: y-sato@idac.tohoku.ac.jp

Received 12 May 2006; Accepted 14 November 2006

Published online in Wiley InterScience (www.interscience.wiley.com.), 26 March 2007.
DOI: 10.1002/jcp.20980

cytoskeleton induces the formation of membrane protrusion such as membrane ruffling (Small et al., 2002). In contrast, RhoA regulates the assembly of contractile acto-myosin filaments. This RhoA-mediated acto-myosin contractile force promotes locomotion of the cell body and the trailing edge (Nobes and Hall, 1999). These organized activities of Rho family small GTPases make the proper cell polarity.

We previously showed that PILSAP did not affect integrin expression, but was involved in adhesion to extracellular matrix proteins (Akada et al., 2002). Here, we extended our analysis to elucidate the molecular mechanism as to how PILSAP regulates adhesion of ECs. Our present analysis revealed that PILSAP takes part in the activation of RhoA in ECs.

Materials and Methods

Materials

The following materials were used: growth factor-reduced Matrigel (Collaborative Research, Bedford, MA); α-minimum essential medium (αMEM), Opti-MEM, Lipofectamine, Superscript II reverse transcriptase, oligo(dT)12–18 primer, and oligofectamine (Gibco BRL, Rockville, MD); anti-RhoA Ab and anti-Rac1 Ab (Santa Cruz Biotechnology, Santa Cruz, CA); Isogen (Nippon Gene, Toyama, Japan); PAR1 agonist peptide (PAR-1 AP) (TFLLR-NH_2, Tocris Cookson, Bristol, UK); Y27632 (EMD Bioscience, San Diego, CA); lysophosphatidic acid (LPA; Biomol Laboratories, Plymouth Meeting, PA); nitrocellulose membranes (Amersham Biosciences, Buckinghamshire, UK); FuGENE 6 Reagent (Roche Diagnostics, Mannheim, Germany); C3 exoenzyme (Calbiochem, La Jolla, CA). Other chemicals were purchased from Sigma (St. Louis, MO).

Cell culture

Mouse endothelial MSS31 cells isolated from mouse spleen microfossils (Yanai et al., 1991) were routinely cultured in αMEM containing 5% fetal bovine serum (5% FBS/αMEM; Oda et al., 1999). MSS31 cells were stably transfected with pcDNA4A (Invitrogen, Carlsbad, CA) empty vector (Mock), Wt-PILSAP or Mut-PILSAP (Yamazaki et al., 2004). Established transfectants in bulk were maintained in 5% FBS/αMEM containing 100 μg/ml of zeocin (Invitrogen). Mut-PILSAP acts as a dominant negative molecule in which glutamate residue 343 is substituted with an alanine (E343A) in the aminopeptidase motif of PILSAP.

Immunofluorescence staining

For the inhibition of RhoA, cells were treated with C3 exoenzyme according to the method described by Minambres et al. (2006). Briefly, C3 exoenzyme (2.5 μg) was precomplexed with FuGENE 6 Reagent (5 μl) in 100 μl of opti-MEM, and C3 exoenzyme complex was added to the cultures. For the inhibition of Rho kinase, cells were incubated in 5% FBS/αMEM on type-I collagen coated dishes for 8 or 10 h with or without Y27632. In addition, cells were cultured in 1% FBS/αMEM prior to inoculation onto type-I collagen coated dishes for 10 h and then stimulated with or without PAR-1 AP (40 μM) or LPA (10 μM).

Thereafter, cells were fixed with 3.8% formaldehyde for 10 min at room temperature and permeabilized with 0.1% Triton X-100 in phosphate buffered saline (PBS). Non-specific binding sites were blocked with 1% bovine serum albumin (BSA) in PBS. Filamentous actin (F-actin) was detected by rhodamine phalloidine (Molecular Probes, Eugene, OR) and focal adhesion complexes were detected by indirect immunofluorescence by using anti-paxillin Ab (Transduction Laboratories, Lexington, KY) and FITC-labeled secondary Ab (Jackson ImmunoResearch, West Grove, PA). Then, cells were observed by confocal microscopy (LSM410, Carl Zeiss Jena GmbH, Jena, Germany).

Cell morphology during movement

Transfected cells were plated onto type-I collagen coated 35 mm dishes for 10 h in 5% FBS/αMEM at a sparse density, so that cells did not affect the movement of each other. Cells were cultured at 37°C in 5% CO_2. Next, cells were photographed by phase-contrast time lapse microscopy in random high-power (200×) fields after additional incubation of 2–6 min.

RhoA and Rac1 activities

Pull-down assay kits (Rho activation assay kit and Cdc42 activation kit, Upstate Biotechnology, Lake Placid, NY) were used to measure RhoA, Rac1 and Cdc42 activities in stable transfectants, leucinethiol (LT), a specific inhibitor of leucine aminopeptidase, treated parental cells or siRNA transfected parental cells. The Cdc42 activation kit includes p21 activated kinase 1 (PAK-1) binding domain agarose. PAK-1 binds both Rac1 and Cdc42 thus; it can measure both Rac1 and Cdc42 activity. Cells were cultured in 1% FBS/αMEM for 24 h and replated in 1% FBS/αMEM on type-I collagen coated dishes for 10 h. In LT treatment experiments, parental cells were plated onto type-I collagen coated dishes for 10 h in 1% FBS/αMEM with or without LT. In some experiments, cells were treated with or without 1% FBS/αMEM containing PAR-1 AP (40 μM) or LPA (10 μM) for 5 min. Cells were extracted with lysis buffer A (25 mM HEPES pH 7.5, 150 mM NaCl, 1% Igepal CA-630, 10 mM $MgCl_2$, 1 mM EDTA, and 10% glycerol). The pull-down of activated RhoA, Rac1, or Cdc42 was performed according to the manufacturer's protocol. A protein assay was performed to equalize the protein amount of each treatment group.

Western blot analysis

The proteins extracted by lysis buffer A or the samples obtained by pull-down assay were separated by SDS–polyacrylamide gel electrophoresis on a 10% gel and then transferred to nitrocellulose membranes (Iwasaka et al., 1996). The membranes were blocked for 1 h at room temperature with Tris-HCl-buffered saline (TBS), pH 7.4, containing 5% skim milk, and then incubated for 1 h at room temperature in TBS containing 0.05% Tween-20 (T-TBS), 1% BSA, and anti-RhoA Ab (1:1,000) or anti-Rac1 Ab (1:1,000). The filters were washed three times with T-TBS and incubated for 1 h with horseradish peroxidase-conjugated protein G (Bio-Rad, Hercules, CA) diluted 1:3,000 in T-TBS. After the filters were washed with T-TBS three times, signal was detected by an enhanced chemiluminescence method with the ECL Western blotting detection kit (Amersham Bioscience). The results were visualized with LAS-1000 (Fuji Film, Tokyo, Japan).

siRNA transfection

RNA interference of the ERAAP gene (identical to PILSAP) was described by Serwold et al. (2002). We generated another siRNA to strengthen the siRNA-mediated knock down of PILSAP. The coding strands of the two pair of siRNA oligonucleotide directed to the 5′ end of mouse PILSAP messenger RNA were 5′-AGCUAGUAAUGGAGACUCATT-3′, 5′-UGAGUCUCCAUUACUAGCUTT-3′ and 5′-CCUCAGCACUCGACUUUCTT-3′, 5′-GAAAGUCAGAGUGCUGAGGTT-3′ and scramble RNAs, the negative control of siRNA, were 5′-AAGAUUCGACGAGCUAUAGTT-3′, 5′-CUAUAGCUCGUCGAAUCUUTT-3′ and 5′-UUAGCCCGUCUACGAAUUUTT-3′, 5′-AAAUUCGUAGACGGGCUAATT-3′. RNA duplexes were denatured in annealing buffer (100 mM NaCl, 50 mM Tris-HCl pH 7.5) at 90°C for 1 min and subsequently annealed at 60°C for 1 h. MSS31 cells were cultured in 5% FBS/αMEM for 24 h, and then oligonucleotides were transfected into cells using oligofectamine according to the manufacturer's instructions. Twenty-four hours

after transfection, MSS31 cells were cultured in 5% FBS/αMEM for 24 h. The gene silencing effect was confirmed by a quantitative real time RT-PCR.

Quantitative real time RT-RCR

Quantitative real time RT-PCR was performed using a Light Cycler System (Roche Diagnostics) as described previously (Shibuya et al., 2006). Total RNA isolated from parental MSS 31 cells was extracted by ISOGEN according to the manufacturer's instructions. RNA was reverse transcribed with AMV reverse transcriptase (Roche Diagnostics) and oligo(dT)12–18 primer according to the manufacturer's instructions. PCR conditions consisted of an initial denaturation step at 95°C for 10 min, followed by 40 cycles of 15 sec at 95°C, 5 sec at 60°C and 15 sec at 72°C. The primer pairs used were: PILSAP 5′-GATGATGGATGGGCTTCTCT-3′ (forward primer) and 5′-GGCTTTTCTCAGTACTAGAC-3′ (reverse primer); mouse β-actin 5′-TCGTGCGTGACATCAAAGAG-3′ (forward primer) and 5′-TGGACAGTGAGGCCAGGATG-3′ (reverse primer). Each mRNA level was measured as a fluorescent signal corrected according to the signal for β-actin.

Network formation

The transfected cells were harvested with 0.25% trypsin and 1 mM EDTA, resuspended in 5% FBS/αMEM with or without Y27632 (10 μM) in a final volume of 1 ml, replated (2×10^5 cells per dish) onto 35 mm dishes coated with Matrigel (700 μl per dish), and incubated at 37°C for 12 h. Cells were observed by phase-contrast microscopy. The length of network structures was quantified with Soft Imaging System Analysis.

Calculations and statistical analysis

The statistical significance of differences in the data was evaluated by the use of unpaired analysis of variance. *P* values were calculated by the unpaired Student *t*-test. $P < 0.05$ was accepted as statistically significant.

Results

PILSAP is involved in F-actin formation during cell adhesion

The consensus HEXXH(18X)E motif is defined as a unique signature for zinc metalloproteinase and glutamate residues are essential for catalytic activity (Hooper, 1994). We previously established a plasmid in which glutamate residue 343 is substituted with an alanine (E343A, namely, HAXXH(18X)E) in the aminopeptidase motif of PILSAP, and this mutant PILSAP acts as a dominant negative molecule (Yamazaki et al., 2004). To investigate the biological function of PILSAP in ECs, we transfected MSS31 cells with empty vector (Mock), wild-type PILSAP (Wt-PILSAP) expressing vector or mutant PILSAP (Mut-PILSAP) expressing vector, and established the respective stable transfectants. Cells were routinely cultured on type-I collagen coated dishes. The most significant change that we found was cell morphology. As shown in Figure 1A, Mut-PILSAP transfectants showed disk-like morphology and lost cell polarity in sparse to subconfluent conditions. Because of this phenotypic change, we examined the actin cytoskeleton organization. Stress fibers were scarcely formed in Mut-PILSAP transfectants (Fig. 1B). In contrast, formation of membrane ruffling was increased but in random directions in Mut-PILSAP transfectants (Fig. 1C).

ECs use at least a type I collagen receptor integrin α2β1, a fibronectin receptor α5β1, and vitronectin receptors αvβ3 and αvβ5 for angiogenesis (Brooks et al., 1994; Collo and Pepper, 1999). Expression of these integrins was unaltered, and identical phenotypic changes were observed when transfectants were plated on fibronectin or vitronectin coated dishes (data not shown).

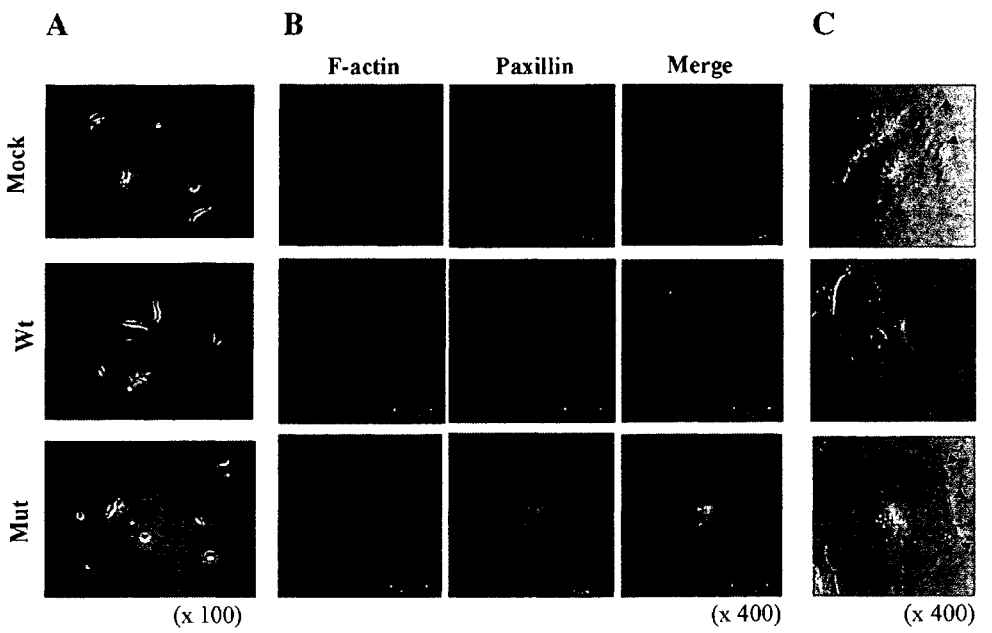

Fig. 1. Involvement of PILSAP in cell shape change, actin organization and membrane ruffling. A: Transfectants were plated onto type-I collagen coated dishes and incubated for 8 h in 5% FBS/αMEM. Cell shape was observed by a phase-contrast microscopy (upper part, 40×, lower part, 100×). B: Transfectants were plated onto type-I collagen coated dishes, and incubated for 8 h in 5% FBS/αMEM, and then stained with rhodamine-phalloidin (red) and anti-paxillin Ab (green). A scale bar indicates 50 μm. C: Cell morphology during movement was observed by time lapse microscopy. Typical pictures are shown here. Arrow heads indicate membrane ruffling.

PILSAP is involved in RhoA activation for EC morphogenesis

As Rho family small GTPases play a pivotal role in actin cytoskeleton reorganization, we examined the activities of RhoA, Rac1 and Cdc42 in transfectants upon cell adhesion. We observed that RhoA activity was attenuated, while Rac1 activity was augmented in Mut-PILSAP transfectants (Fig. 2A). Cdc42 activity was hardly detected (data not shown). Involvement of PILSAP in RhoA activation was confirmed by two additional treatments. We previously showed that PILSAP was highly sensitive to LT, but was insensitive to puromycin (Miyashita et al., 2002). LT inhibited spreading of MSS31 cells upon extracellular matrix such as type1 collagen, fibronectin and vitronectin (Akada et al., 2002). Here we examined whether LT influenced RhoA activity. As shown in Figure 2B, LT inhibited RhoA activation in parental MSS31 cells when added to the medium. Moreover PILSAP siRNAs, which knocked down to 16% of the control level of PILSAP mRNA (Fig. 2D), decreased RhoA activity of parental MSS31 cells (Fig. 2C).
RhoA regulates cell contractility through its downstream Rho kinase (Alblas et al., 2001). To further confirm the involvement of RhoA activity in EC morphogenesis, we employed specific RhoA inhibitor, C3 exoenzyme, or a Rho kinase inhibitor, Y27632. When parental MSS31 cells were treated with C3 exoenzyme or Y27632, cells exhibited cell-shape changes identical to that in Mut-PILSAP transfectants (Fig. 3A,B).
ECs form network-like structures when plated on Matrigel. This network formation was aborted in Mut-PILSAP transfectants, or by the treatment of Wt-PILSAP transfectants with Y27632 (Fig. 4). These results indicate that PILSAP is involved in RhoA activation for proper morphogenesis and organization of ECs.

PILSAP is involved in RhoA activation via G-protein coupled receptors

During the maintenance of transfectants in culture, we noticed that Mut-PILSAP transfectants showed delayed cell shrinkage upon trypsin/EDTA treatment for cell harvest. We reasoned this delay of cell shrinkage was due to impaired RhoA activation. Indeed, when transfectants were pretreated with Y27632, cell shrinkage upon trypsin/EDTA treatment was inhibited in Mock or Wt-PILSAP transfectants (data not shown). Trypsin activates proteinase-activated receptors (PARs). PARs belong to the G-protein coupled receptors (GPCRs), and ECs express PAR1 and PAR2 (Brass and Molino, 1997). Western blot analysis revealed that protein levels of PAR1 and PAR2 were identical between the three transfectants (data not shown). It was previously reported that PAR1 or PAR2 agonist induced RhoA activation in HUVEC (Vouret-Craviari et al., 2003). Here we used the PAR1 AP to induce RhoA activity in our system. There was no significant difference in the basal level of RhoA activity between transfectants. However when transfectants were treated with the PAR1 AP, RhoA activation was almost completely abolished in Mut-PILSAP transfectants (Fig. 5A). Moreover, with respect to actin reorganization, PAR1 AP

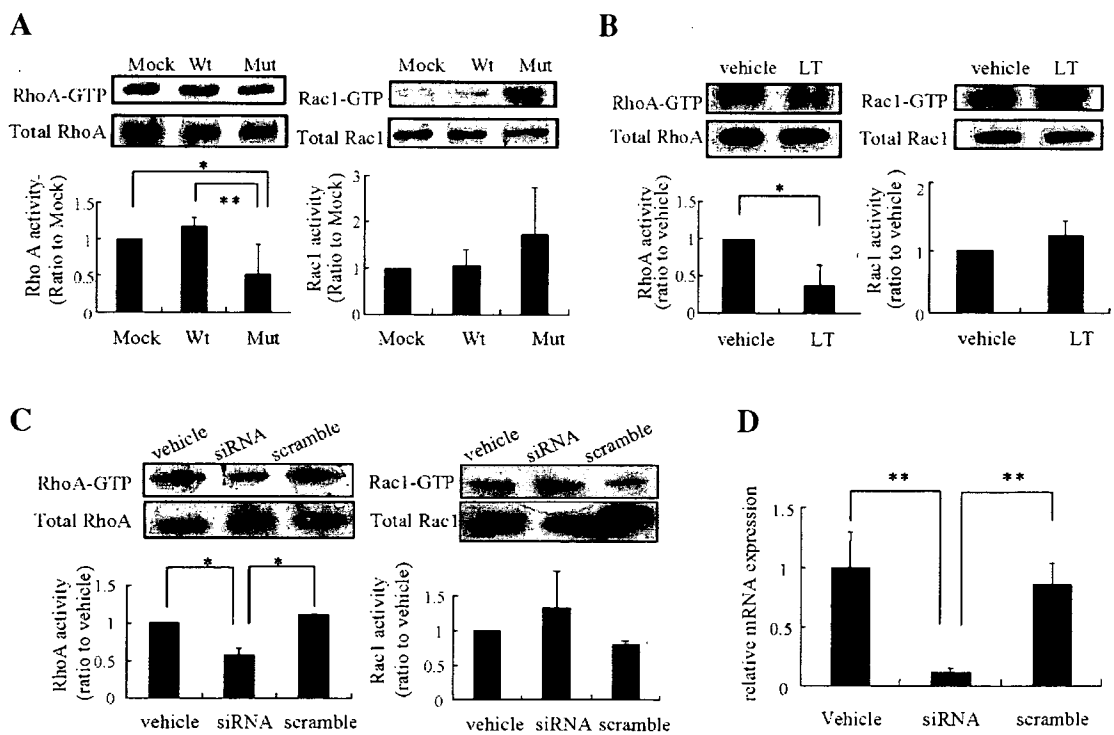

Fig. 2. Involvement of PILSAP in RhoA activation. A: Transfectants were incubated on type-1 collagen for 10 h in 1% FBS/αMEM. Then, RhoA and Rac1 activities were determined. B: Parental MSS31 cells were incubated on type-1 collagen for 10 h in 1% FBS/αMEM with or without LT (10 μmol/L). Next, RhoA and Rac1 activities were determined. GTP-RhoA or GTP-Rac1 was quantified by density and normalized to that of total RhoA or total Rac1. The values are expressed as the mean ± SD from three independent experiments; *$P < 0.05$, **$P < 0.01$. C: Parental MSS31 cells were transfected with PILSAP siRNA and incubated in 1% FBS/αMEM for 24 h. Then, transfectants were plated onto type-1 collagen coated dishes and incubated for 10 h. Next, RhoA and Rac1 activities were determined. The values are expressed as the mean ± SD from two independent experiments; *$P < 0.05$. D: The gene silencing effect of PILSAP siRNA was confirmed by quantitative real time RT-PCR. The values are expressed as the mean ± SD from three samples; **$P < 0.01$.

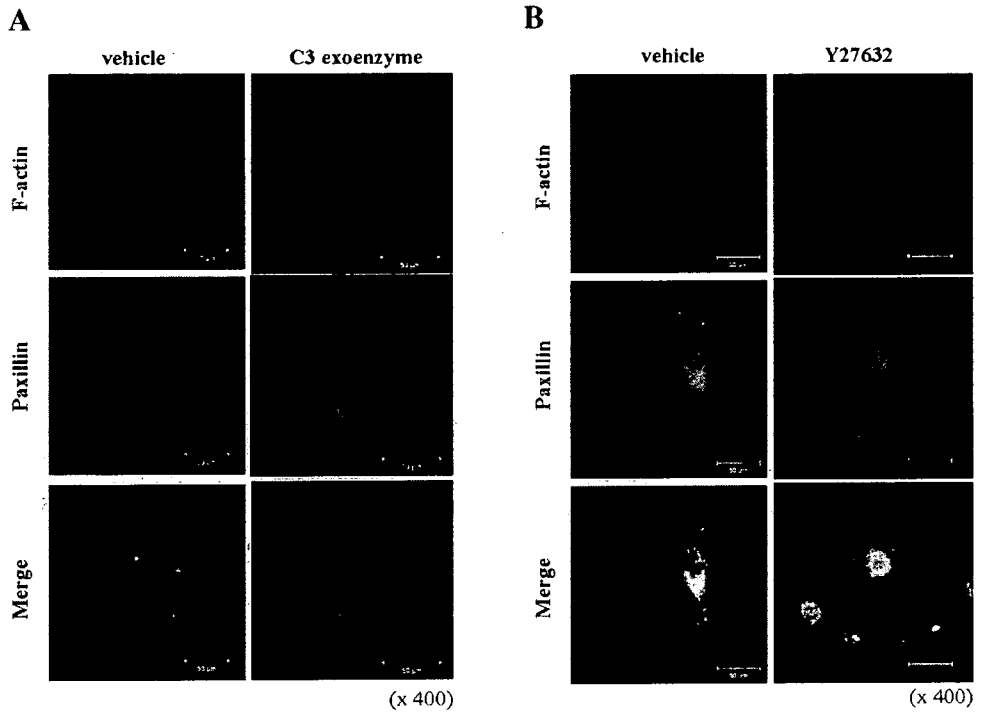

Fig. 3. Effects of RhoA and Rho kinase inhibitors on cell morphology. A: Parental MSS31 cells were plated onto type-I collagen coated dishes and incubated for 1 h in 5% FBS/αMEM. Next, cells were treated with or without C3 exoenzyme precomplexed with FuGENE 6 Reagent for additional 7 h. Cells were then stained with rhodamine-phalloidin (red) and anti-paxillin Ab (green). B: Parental MSS31 cells were plated onto type-I collagen coated dishes and incubated for 8 h in 5% FBS/αMEM. Next, cells were treated with or without Y27632 (10 μmol/L) for 30 min. Cells were then stained with rhodamine-phalloidin (red) and anti-paxillin Ab (green).

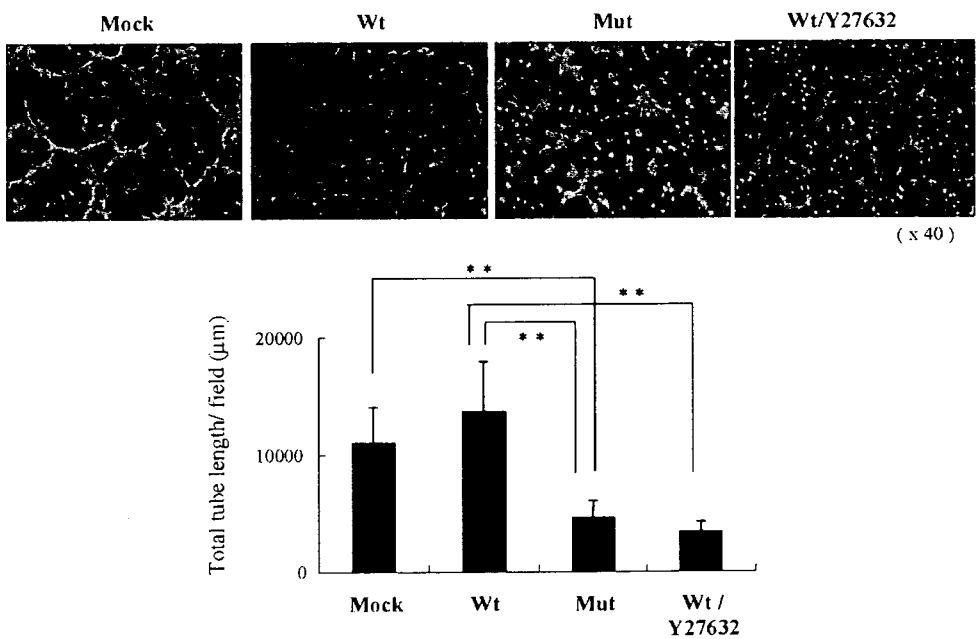

Fig. 4. Role of Rho kinase in alteration of network formation mediated by PILSAP. Transfectants were plated onto Matrigel and incubated in 5% FBS/αMEM for 12 h. In some experiments, cells were incubated in the presence of Y27632 (10 μmol/L). The total length of network structures per field (×40 magnification) was quantified with Soft Imaging System Analysis. The values are expressed as the mean ± SD of four fields; $^{**}P < 0.01$.

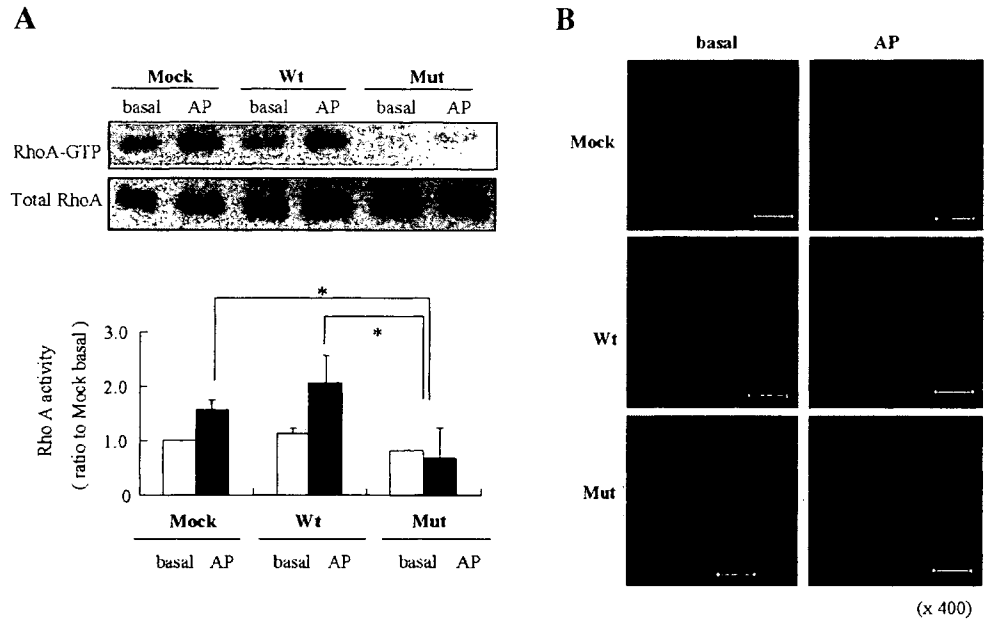

Fig. 5. Involvement of PILSAP in RhoA activation upon stimulation through PARs. A: Transfectants were incubated on type-I collagen for 10 h in 1% FBS/αMEM, and then treated with or without PAR-1 AP (AP) (40 μmol/L) for 5 min. Next, RhoA activity was determined. GTP-RhoA was quantified by density and normalized to that of total RhoA. The values are expressed as the mean ± SD from four independent experiments; *$P < 0.05$. B: Transfectants were incubated on type-I collagen for 10 h in 1% FBS/αMEM, and then treated with or without PAR-1 AP (AP) (40 μmol/L) for 5 min. Subsequently, they were fixed and stained with rhodamine-phalloidine. A scale bar indicates 50 μm.

induced stress fiber formation in Mock or Wt-PILSAP transfectants but not in Mut-PILSAP transfectants (Fig. 5B). LPA binds to the LPA receptor and activates RhoA for F-actin formation in ECs (Panetti, 2002). When transfectants were treated with LPA, RhoA activation was significantly lower in Mut-PILSAP transfectants (Fig. 6A). Stress fiber formation was not induced by LPA in Mut-PILSAP transfectants (Fig. 6B). Moreover, LT or PILSAP siRNA inhibited LPA-stimulated activation of RhoA in parental MSS31 cells (Fig. 7A,B). These results indicate that the involvement of PILSAP in RhoA

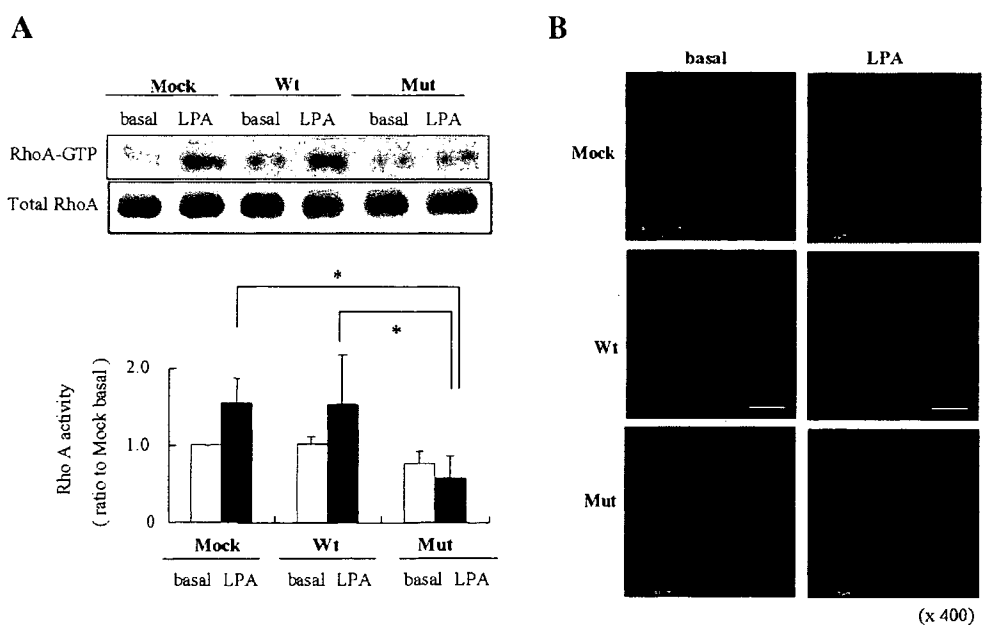

Fig. 6. Involvement of PILSAP in RhoA activation upon LPA stimulation. A: Transfectants were incubated on type-I collagen for 10 h in 1% FBS/αMEM, and then treated with or without LPA (10 μmol/L) for 5 min. Next, RhoA activity was determined. GTP-RhoA was quantified by density and normalized to that of total RhoA. The values are expressed as the mean ± SD from four independent experiments; *$P < 0.05$. B: Transfectants were incubated on type-I collagen for 10 h in 1% FBS/αMEM, and then treated with or without LPA (10 μmol/L) for 5 min. Subsequently, they were fixed and stained with rhodamine-phalloidine. A scale bar indicates 50 μm.

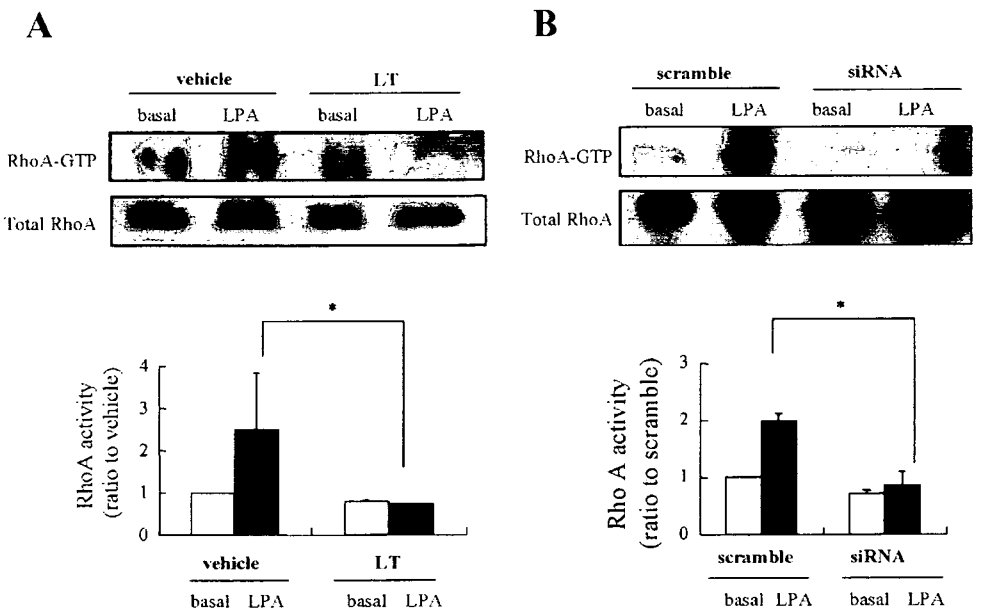

Fig. 7. Effect of PILSAP inhibition or knockdown on RhoA activation upon LPA stimulation. A: Parental MSS31 cells were incubated on type-I collagen for 10 h in 1% FBS/αMEM with or without LT (10 μmol/L). Next, cells were treated with or without LPA (10 μmol/L) for 5 min, and RhoA activity was determined. The values are expressed as the mean ± SD from three independent experiments; *$P < 0.05$. B: Parental MSS31 cells were transfected with PILSAP siRNA and cells were incubated in 1%FBS/αMEM for 24 h. Then, transfected cells were plated onto type-I collagen coated dishes and incubated for 10 h. Next, cells were treated with or without LPA (10 μmol/L) for 5 min, and RhoA activity was determined. GTP-RhoA was quantified by the density and normalized to that of total RhoA. The values are expressed as the mean ± SD from two independent experiments; *$P < 0.05$.

activation is not specific during cell adhesion but rather a general component.

Discussion

The present study reveals for the first time that PILSAP takes part in the regulation of RhoA activation in ECs. We have previously reported that PILSAP is involved in S6K activation by catalyzing its upstream partner PDK1 (Yamazaki et al., 2004). Thus, RhoA is noted as another target of PILSAP among the intracellular signaling pathways.

Amid three representative Rho family small GTPases, Rac and cdc42 stimulate protrusion formation at the leading edge and cause membrane ruffle formation, a remodeling of cortical actin (Lauffenburger and Horwitz, 1996; Doughman et al., 2003), whereas RhoA stimulates F-actin formation for contraction of the cell body and the trailing edge. Cdc42 regulates cell migration direction (Raftopoulou and Hall, 2004). The phenotype of Mut-PILSAP transfectants with defective activation of RhoA was quite logical, as they showed aborted F-actin formation and cell polarity.

The importance of RhoA for EC organization during angiogenesis has been documented by Hoang et al. (2004). In that report, constitutive active RhoA stimulated ECs to form vessels with functional lumens while dominant negative RhoA impaired assembly of ECs for neovessel formation. Consistent with that report, network formation by mouse endothelial MSS31 cells on Matrigel was prevented by Mut-PILSAP transfection as well as in the presence of Rho kinase inhibitor (Y27632).

Rho family small GTPases are activated by various extracellular signals through transmembrane proteins including integrins and GPCRs (Karnoub et al., 2004). Among various integrins, β1 integrins support the activation of RhoA, which is associated with a random mode of cell migration (Danen et al., 2005).

GPCRs exhibit a common structural motif consisting of seven membrane-spanning regions (Dohlman et al., 1987), and can be activated by a diverse array of external stimuli, including vasoactive polypeptides, chemoattractants, neurotransmitters, hormones, phospholipids, odorants, and taste ligands (Fukuhara et al., 2001). In general, agonists provoke rapid conformational changes in transmembrane α helices, resulting in exposure of previously masked G protein binding sites in intracellular loops (Altenbach et al., 1996; Bourne, 1997; Wess, 1997). This causes the exchange of GDP for GTP bound to G protein α-subunits or βγ-complexes, and then the initiation of the intracellular signaling response by acting on a variety of effecters. In our study, PILSAP-dependent RhoA activation in ECs is shown not only during cell adhesion but also upon stimulation of PARs or LPA receptor. Thus, PILSAP is rather a general player for RhoA activation in ECs.

Rho family small GTPases act as molecular switches by cycling between GTP- and GDP-bound states. The GTP/GDP cycle is tightly regulated by 3 distinct families of proteins; guanine nucleotide exchange factors (GEFs), GTPase-activating proteins (GAPs) and the guanine nucleotide dissociation inhibitors (GDIs) (Symons and Settleman, 2000). Among them, GEFs activate GTPases by catalyzing the exchange of GDP for GTP, thereby increasing the levels of GTP-bound forms (Donovan et al., 2002; Schmidt and Hall, 2002). More than 70 GEFs have been isolated for Rho family small GTPases (RhoGEFs; Rossman et al., 2005). Whereas many RhoGEFs are highly promiscuous and activate plural Rho family small GTPases, some show activity restricted to a single GTPase (Karnoub et al., 2004). p115-RhoGEF is regarded as a prototype of such RhoA specific GEFs (Hart et al., 1996; Holinstat et al., 2003). Since the requirement of PILSAP was selective to RhoA activation, we employed p115-RhoGEF as a model in our system. Whereas expression of p115-RhoGEF of the mRNA and protein levels were equivalent among Mock, Wt-PILSAP

and Mut-PILSAP transfectants, the GDP/GTP exchanging activity of p115-RhoGEF was significantly lower in Mut-PILSAP transfectants (data not shown).

PARs constitute a subclass of GPCRs that convert extracellular serine protease activity to intracellular signaling events. Proteolysis of PARs results in the cleavage of specific sites in the extracellular domain and formation of a new N-terminus that functions as a tethered ligand. Four types (PAR1, PAR2, PAR3, and PAR4) of this receptor class have been identified in mammals. PAR1, 3 and 4 are activated essentially by thrombin, whereas PAR2 can be activated by trypsin (Cottrell et al., 2002). ECs express at least PAR1 and PAR2 (Brass and Molino, 1997). RhoA-GTP was robustly activated by PAR1 stimulation, but only weakly by PAR2 stimulation by receptor-selective concentration of agonist peptides, and activity of RhoA-GTP and myosin light chain phosphorylation is required for PAR1-mediated monolayer permeability (Klarenbach et al., 2003). Moreover, recent studies have revealed that PARs are involved in vascular development and other biological processes including vascular remodeling (Barnes et al., 2004). The LPA receptor belongs to the endothelial differentiation gene (EDG), also known as the sphingosine 1-phosphate (S1P) receptor family of GPCRs. S1P has the potential to act through endothelial EDG1, EDG3 and probably EDG5, whereas LPA is limited to EDG2 and/or EDG4 (Panetti, 2002). LPA and S1P are important regulators of the vascular system, including angiogenesis and vascular permeability (Panetti, 2002). Thus, the involvement of PILSAP in downstream signaling of PARs and LPA receptor indicate that PILSAP should function in the broad range of vascular pathophysiology.

In summary, the present study reveals for the first time that PILSAP takes part in the regulation of RhoA activation in ECs. This data should provide clues to devise a novel strategy for the regulation of EC function during various processes including angiogenesis.

Acknowledgments

This work was supported by grant-in-aid for Scientific Research on Priority Areas of the Japanese Ministry of Education, Science, Sports and Culture from the Ministry of Education, Science, Sports and Culture of Japan (16022205 and 17014006).

Literature Cited

Akada T, Yamazaki T, Miyashita H, Niizeki O, Abe M, Sato A, Satomi S, Sato Y. 2002. Puromycin insensitive leucyl-specific aminopeptidase (PILSAP) is involved in the activation of endothelial integrins. J Cell Physiol 193:253–262.

Alblas J, Ulfman L, Hordijk P, Koenderman L. 2001. Activation of RhoA and ROCK are essential for detachment of migrating leukocytes. Mol Biol Cell 12:2137–2145.

Altenbach C, Yang K, Farrens DL, Farahbakhsh ZT, Khorana HG, Hubbell WL. 1996. Structural features and light-dependent changes in the cytoplasmic interhelical E-F loop region of rhodopsin: A site-directed spin-labeling study. Biochemistry 35:12470–12478.

Barnes JA, Singh S, Gomes AV. 2004. Protease activated receptors in cardiovascular function and disease. Mol Cell Biochem 263:227–239.

Bourne HR. 1997. How receptors talk to trimeric G proteins. Curr Opin Cell Biol 9:134–142.

Brass LF, Molino M. 1997. Protease-activated G protein-coupled receptors on human platelets and endothelial cells. Thromb Haemost 78:234–241.

Brooks PC, Clark RA, Cheresh DA. 1994. Requirement of vascular integrin αvβ3 for angiogenesis. Science 264:569–571.

Collo G, Pepper MS. 1999. Endothelium cell integrin α5β1 expression is modulated by cytokines and during migration in vitro. J Biol Chem 270:26931–26939.

Cottrell GS, Coelho AM, Bunnett NW. 2002. Protease-activated receptors: The role of cell-surface proteolysis in signaling. Essays Biochem 38:169–183.

Danen EH, van Rheenen J, Franken W, Huveneers S, Sonneveld P, Jalink K, Sonnenberg A. 2005. Integrins control motile strategy through a Rho-cofilin pathway. J Cell Biol 169:515–526.

Dohlman HG, Caron MG, Lefkowits RJ. 1987. A family of receptors coupled to guanine nucleotide regulatory proteins. Biochemistry 26:2657–2664.

Donovan S, Shannon KM, Bollag G. 2002. GTPase activation proteins: Critical regulators of intracellular signaling. Biochem Biophys Acta 1602:23–45.

Doughman RL, Firestone AJ, Wojtasiak ML, Bunce MW, Anderson RA. 2003. Membrane ruffling requires coordination between type I alpha phosphatidylinositol phosphate kinase and Rac signaling. J Biol Chem 278:23036–23045.

Fukuhara S, Chikumi H, Gutkind JS. 2001. RGS-containing RhoGEFs: The missing link between transforming G proteins and Rho? Oncogene 20:1661–1668.

Hart MJ, Sharma S, elMasry N, Qiu RG, McCabe P, Polakis P, Bollag G. 1996. Identification of a novel guanine nucleotide exchanging factor for the Rho GTPase. J Biol Chem 271:25452–25458.

Hoang MV, Whelan MC, Senger DR. 2004. Rho activity critically and selectively regulates endothelial cell organization during angiogenesis. Proc Natl Acad Sci USA 17:1874–1879.

Holinstat M, Mehta D, Kozasa T, Minshall RD, Malik AB. 2003. Protein kinase Cα-induced p115 RhoGEF phosphorylation signals endothelial cytoskeletal rearrangement. J Biol Chem 278:28793–28798.

Hooper NM. 1994. Families of zinc metalloproteases. FEBS Lett 354:1–6.

Iwasaka C, Tanaka K, Abe M, Sato Y. 1996. Ets-1 regulates angiogenesis by inducing the expression of urokinase-type plasminogen activator and matrix metalloproteinase-1 and the migration of vascular endothelial cells. J Cell Physiol 169:522–531.

Karnoub AE, Symous M, Campbell SL, Der CJ. 2004. Molecular basis for Rho GTPase signaling specificity. Breast Cancer Res Theat 84:61–71.

Klarenbach SW, Chipiuk A, Nelson RC, Hollenberg MD, Murray AG. 2003. Differential actions of PAR2 and PAR1 in stimulating human endothelial cell exocytosis and permeability: The role of Rho-GTPases. Circ Res 92:272–278.

Lauffenburger DA, Horwitz AF. 1996. Cell migration: A physically integrated molecular process. Cell 84:359–369.

Li S, Huang NF, Hsu S. 2005. Mechanotransduction in endothelial cell migration. J Cell Biochem 96:1110–1126.

Minambres R, Guasch RM, Perez-Arago A, Guerri C. 2006. The RhoA/ROCK-I/MLC pathway is involved in the ethanol-induced apoptosis by anoikis in astrocytes. J Cell Sci 119:271–282.

Miyashita H, Yamazaki T, Akada T, Niizeki O, Ogawa M, Nishikawa S, Sato Y. 2002. A mouse orthologue of puromycin-insensitive leucyl-specific aminopeptidase is expressed in endothelial cells and plays an important role in angiogenesis. Blood 99:3241–3249.

Niizeki O, Miyashita H, Yamasaki T, Akada T, Abe M, Yoshida N, Watanabe T, Yoshimatsu H, Sato Y. 2004. Transcriptional regulation of angiogenesis-related puromycin-insensitive leucyl-specific aminopeptidase in endothelial cells. Arch Biochem Biophys 424:63–71.

Nobes CD, Hall A. 1999. Rho GTPase control polarity, protrusion, and adhesion during cell movement. J Cell Biol 144:1235–1244.

Oda N, Abe M, Sato Y. 1999. ETS-1 converts endothelial cells to the angiogenic phenotype by inducing the expression of matrix metalloproteinases and integrin β3. J Cell Physiol 178:121–132.

Panetti TS. 2002. Differential effects of sphingosine 1-phosphate and lysophosphatidic acid on endothelial cells. Biochem Biophys Acta 1582:190–196.

Raftopoulou M, Hall A. 2004. Cell migration: Rho GTPases lead the way. Dev Biol 265:23–32.

Rossman KL, Der CJ, Sondek J. 2005. GEF means go: Turning of RHO GTPase with guanine nucleotide-exchanging factors. Nat Rev Mol Cell Biol 6:167–180.

Schmidt A, Hall A. 2002. Guanine nucleotide exchange factors for Rho GTPases: Turning on the switch. Gene Dev 16:1587–1609.

Serwold T, Gonzalez F, Kim J, Jacob R, Shastri N. 2002. ERAAP customizes peptides for MHC class I molecules in the endoplasmic reticulum. Nature 419:480–483.

Sheetz MP, Felsenfeld DP, Galbraith CG. 1998. Cell migration: Regulation of force on extracellular-matrix-integrin complexes. Trends Cell Biol 8:51–54.

Shibuya T, Watanabe K, Yamashita H, Shimizu K, Miyashita H, Abe M, Moriya T, Ohta H, Sonoda H, Shimosegawa T, Tabayashi K, Sato Y. 2006. Isolation and characterization of vasohibin-2 as a homologue of VEGF-inducible endothelium-derived angiogenesis inhibitor vasohibin. Arterioscler Thromb Vasc Biol 26:1051–1057.

Small JV, Stradal T, Vignal E, Rottner K. 2002. The lamellipodium: Where motility begins. Trends Cell Biol 12:112–120.

Symons M, Settleman J. 2000. Rho family GTPases: More than simple switches. Trends Cell Biol 10:415–419.

Taylor A. 1993. Aminopeptidases: Structure and function. FASEB J 7:290–298.

Vouret-Craviari V, Grall D, Van Obberghen-Schilling E. 2003. Modulation of Rho GTPase activity in endothelial cells by selective proteinase-activated receptor (PAR) agonists. J Thromb Haemost 5:1103–1111.

Wess J. 1997. G-protein-coupled receptors: Molecular mechanisms involved in receptor activation and selectivity of G-protein recognition. FASEB J 11:346–354.

Yamazaki T, Akada T, Niizeki O, Suzuki T, Miyashita H, Sato Y. 2004. Puromycin-insensitive leucyl-specific aminopeptidase (PILSAP) binds and catalyzes PDK1, allowing VEGF-stimulated activation of S6K for endothelial cell proliferation and angiogenesis. Blood 104:2345–2352.

Yanai N, Satoh T, Obinata M. 1991. Endothelial cells create a hematopoietic inductive microenvironment preferential to erythropoiesis in the mouse spleen. Cell Struct Funct 16:87–93.

The Vasohibin Family

A Negative Regulatory System of Angiogenesis Genetically Programmed in Endothelial Cells

Yasufumi Sato, Hikaru Sonoda

Abstract—Biological phenomena are under the precise control by the genome. For the regulation of angiogenesis, proangiogenic genes such as VEGFs and angiopoietins are highly conserved, act specifically on endothelial cells, and play a fundamental role. In this sense, nature should prepare specific antiangiogenic genes as well. However, this counterpart of genomic regulation of angiogenesis remains to be established. We recently isolated a novel endothelium-derived angiogenesis inhibitor and named it vasohibin. Vasohibin is dominantly expressed in endothelial cells, induced by the stimulation with VEGF or FGF-2, and selectively affects on endothelial cells and inhibits angiogenesis. Although the mechanism of how vasohibin inhibits angiogenesis remains to be elucidated, our discovery of vasohibin as an endothelium-derived VEGF-inducible angiogenesis inhibitor should shed light on the genomic basis of the negative regulation of angiogenesis. (*Arterioscler Thromb Vasc Biol.* 2007;27:37-41.)

Key Words: endothelial cell ■ angiogenesis inhibitor ■ VEGF ■ negative feedback

Blood vessels are one of the most quiescent tissues in the body, but have the capacity to form neovessels under certain conditions. Angiogenesis, ie, the formation of neovessels from existing ones, is a key event in various processes that takes place under physiological and pathologic conditions. Physiological conditions include embryonic development, reproduction, and wound healing; whereas pathologic conditions include cancers, proliferative retinopathy, and rheumatoid arthritis. Angiogenesis consist of multiple sequential steps: detachment of mural pericytes for vascular destabilization, extracellular matrix degradation by endothelial proteases, migration of ECs, proliferation of ECs, tube formation by ECs, and reattachment of pericytes for vascular stabilization.[1]

The local balance between angiogenesis stimulators and inhibitors regulates angiogenesis. Understanding of the mechanism of angiogenesis regulation has advanced significantly since the discovery of endothelium-specific proangiogenic factors, namely vascular endothelial growth factor (VEGF) and angiopoietins (Ang) family proteins. VEGFs bind to specific VEGF receptors (VEGFRs), while Angs bind to a tyrosine kinase receptor having Ig and EGF homology domains (TIE) receptor expressed exclusively in the endothelium. Among the VEGF family members, VEGF-A is the most important factor for angiogenesis, stimulating protease synthesis, migration, and proliferation of endothelial cells (ECs), and most of the VEGF-A–mediated signals are transduced via VEGFR-2.[2] TIE-2–mediated signals determine vascular maturation by the pericyte attachment. Amid Ang family members (Ang 1–4), Ang-1 and Ang-3/4 are agonistic ligands, whereas Ang-2 is a very weak ligand and acts as an antagonist of TIE-2 receptor.[3] Ang3 (mouse) and Ang4 (human) are interspecies orthologs.[4]

Various molecules are listed as angiogenesis inhibitors.[5] Most of them, such as pigment epithelium derived factor (PEDF), platelet factor 4, angiostatin, and endostatin, are extrinsic to ECs. In addition, ECs themselves have the capacity to express some angiogenesis inhibitors, eg, soluble VEGFR-1 (sVEGFR-1), vascular endothelial growth inhibitor (VEGI), Down syndrome critical region gene 1 (DSCR1), and vasohibin.

The VEGFR-1 gene encodes for both the full-length receptor and a soluble form. sVEGFR-1 carries 6 Ig-like domains as well as a 31-amino-acid stretch derived from intron 13.[6] sVEGFR-1 can be distinguished from the other angiogenesis inhibitors because of its specific activity. It is able to bind specifically VEGF-A as well as VEGF-B and PlGF with high affinities, and functions as a decoy receptor by sequestering them.[6] sVEGFR1 cannot inhibit angiogenesis stimulated by other angiogenic factors such as fibroblast growth factor 2 (FGF-2) or hepatocyte growth factor (HGF) because of its binding specificity. The regulation of the expression of sVEGFR-1 is yet to be characterized.

VEGI is a novel member of the tumor necrosis factor (TNF) family identified from the human umbilical vein endothelial cell (HUVECs) cDNA library.[7] VEGI is a type II

Original received August 21, 2006; final version accepted October 5, 2006.

From the Department of Vascular Biology (Y.S.), Institute of Development, Aging, and Cancer, Tohoku University, Sendai, and the Discovery Research Laboratories (H.S.), Shionogi & Co Ltd, Osaka, Japan.

Correspondence to Yasufumi Sato, Department of Vascular Biology, Institute of Development, Aging, and Cancer, Tohoku University, 4-1 Seiryo-machi, Aoba-ku, Sendai 980-8575, Japan. E-mail y-sato@idac.tohoku.ac.jp

Arterioscler Thromb Vasc Biol. is available at http://www.atvbaha.org

DOI: 10.1161/01.ATV.0000252062.48280.61

transmembrane protein composed of 174 amino acid residues. Unlike other members of the TNF family, VEGI is expressed predominantly in ECs,[7] but importantly, the effect of VEGI is not selective to ECs, and inhibits proliferation of various caner cells as well.[8] The expression of VEGI is regulated mainly by transcription factor NF-κB in parallel with other inflammatory cytokines.[9]

DSCR1 and vasohibin are VEGF-inducible molecules in ECs.[10] DSCR1 is a cytoplasmic protein and is shown to act as an endogenous calcineurin inhibitor,[11] and because of this property, DSCR1 is thought to inhibit angiogenesis.[12] Indeed, overexpression of DSCR1 in ECs inhibited angiogenesis.[13] However, our analysis revealed that specific knockdown of DSCR1 in ECs inhibited angiogenesis.[14] Moreover, our subsequent analysis showed that DSCR1 bind not calcineurin but also Raf-1.[15] Thus, the role of DSCR1 in angiogenesis may not be simple.

Vasohibin and its homologue vasohibin-2 are the most recently identified angiogenesis inhibitors.[16,17] This review will focus on the vasohibin family, a negative regulatory system of angiogenesis genetically programmed in endothelial cells.

Vasohibin

Isolation

DNA microarray analysis was used to identify VEGF-inducible genes in ECs.[10] Among 7267 human sequences, 97 were induced more than 2-fold by VEGF stimulation in HUVECs at the 24 hour time point. Of these 97 sequences, 11 were uncharacterized in terms of their biological function, and we could isolate 1 of these11 genes that had antiangiogenic activity, and named it vasohibin.[16] Human vasohibin protein is composed of 365 amino acid residues, without any detectable glycosilation. A cluster of basic amino acids was present in the C-terminal region, but neither a classical secretion signal sequence nor any other functional motif was found among these amino acid sequences by the database search. The lack of classical signal sequence suggests that vasohibin is an unconventional secretory protein.

Initially the antiangiogenic activity of vasohibin was shown using the in vitro Matrigel assay.[16] Recombinant vasohibin protein inhibited the spontaneously formed network-like structures of HUVECs when plated on Matrigel. The antiangiogenic activity of vasohibin was then further determined by 3 independent in vivo assays When matrigel mixed with VEGF with or without vasohibin protein was inoculated subcutaneously to mice, vasohibin inhibited the VEGF-stimulated angiogenesis. However, vasohibin did not inhibit phosphorylation of VEGFRs in HUVECs.[16] Moreover, the "Miles assay" revealed that vasohibin exhibited no inhibitory effect on VEGF-stimulated acute vascular permeability (unpublished observation, 2005). Indicating that vasohibin is not merely an antagonist of VEGF.

When vasohibin was applied to pellets containing fibroblast growth factor (FGF)-2 in a mouse corneal micropocket assay, vasohibin inhibited FGF-2–stimulated angiogenesis.[16] Introduction of the vasohibin gene into a replication-defective adenovirus vector, and applied it to chicken chorioallantoic membrane (CAM) assay, the adenovirus vector encoding vasohibin abrogated the vessel formation whereas the control adenovirus vector encoding β-galactosidase (AdLacZ) did not.[16] All these data implicate that the antiangiogenic effect of vasohibin is not restricted to VEGF-stimulated angiogenesis. The mechanism as to how vasohibin inhibits angiogenesis remains to be elucidated.

Expression Profile

The expression profile of vasohibin was examined in both in vitro and in vivo. In vitro, vasohibin was predominantly expressed in ECs. The expression in ECs was induced not only by VEGF but also by FGF-2. However, human aortic smooth muscle cells (HASMCs) expressed vasohibin weakly, and platelet derived growth factor (PDGF) modestly increased its expression. In addition, fibroblasts did express very low levels of vasohibin, but was unresponsive to the FGF-2 stimulation. Vasohibin expression was not observed in keratinocytes under either basal or EGF-stimulated conditions.[16]

Inflammation often associates pathological angiogenesis. Our analysis revealed that inflammatory cytokines such as TNFα, interleukin (IL)-1β, and interferon (IFN)γ reduced the VEGF-induced expression of vasohibin in ECs.[16,18] The effect of IL-1β was comparable to that of TNFα, whereas the effect of IFNγ was less pronounced. Hypoxia is known to act as a trigger of both physiological and pathological angiogenesis by inducing VEGF. Hypoxia did not affect the basal expression of vasohibin in ECs. However, hypoxia did inhibit the VEGF-stimulated vasohibin mRNA expression, as well as vasohibin protein synthesis in ECs.[16]

Northern blot analysis of the samples from various tissues revealed that vasohibin was expressed in the brain, and to a lesser extent, in the heart and kidney in the adult.[16] Moreover, a robust expression of vasohibin was demonstrated in the placenta and various developing organs of the human embryo.[16] Furthermore, immunohistochemical analysis revealed that vasohibin was present only in ECs of the human placenta and developing organs in embryo.[16,17] Thus vasohibin is thought to be a molecule selectively expressed in ECs during angiogenesis.

Signals for the Induction of Vasohibin in ECs

The intracellular signaling for the induction of vasohibin in HUVECs by VEGF was characterized using blocking anti-VEGFRs mAbs to test which receptor was involved in the induction of vasohibin.[18] Anti–VEGFR-2 antibodies but not anti–VEGFR-1 antibodies inhibited the VEGF-stimulated induction of vasohibin. The downstream intracellular signaling pathways of VEGFR-2 for the induction of vasohibin were further investigated. GF109203X, a broad-spectrum inhibitor of protein kinase C (PKC), strongly inhibited the increase of vasohibin mRNA and protein in response to VEGF, which was in line with the observation that Phorbol 12-myristate 13-acetate (PMA), an activator of PKC, enhanced the expression of vasohibin in HUVECs. Selective PKC isoform inhibitors were used to clarify which PKC isoforms were involved in the upregulation of vasohibin. Rottlerin, a specific inhibitor of PKCδ, completely blocked

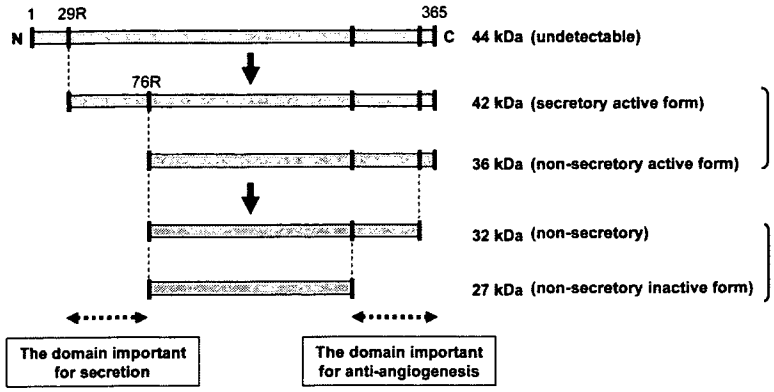

Figure 1. Posttranslational processing, secretion, and biological activity of vasohibin-1. Forty-four-kDa full-length vasohibin-1 cannot be detected. Four different forms of vasohibin-1 are generated after the translation. Forty-two-kDa vasohibin-1 is the major secretory form with antiangiogenic activity. N terminus region is important for secretion, whereas C terminus region is important for antiangiogenesis. The antiangiogenic activity of 32-kDa form is not determined.

the upregulation of vasohibin, whereas Gö6976, a specific inhibitor of PKCα, and HBDDE, an inhibitor of PKCα and PKCγ, partially inhibited it. Hispidin, a specific inhibitor of PKCβ, did not affect the upregulation of vasohibin.[18] From these results it is concluded that PKCδ transduced a principal signal for the upregulation of vasohibin through VEGF. FGF-2 increased the expression of vasohibin in ECs to a level comparable to that obtained with VEGF, and rottlerin again completely blocked FGF-2–stimulated upregulation of vasohibin.[18] Accordingly, the principal signaling pathways for the induction of vasohibin by 2 representative angiogenic growth factors considerably overlap. PKC-δ is known to be a transducer of antiangiogenic signals in ECs.[19] Thus, vasohibin can be a downstream effecter of PKC-δ in ECs for angiogenesis inhibition.

Actinnomycin D treatment did not change the decay of VEGF-induced vasohibin mRNA.[18] Thus, the increase of vasohibin mRNA by VEGF is not determined by mRNA stability. However, when cycloheximide was added, the expression of vasohibin mRNA was completely abolished in both basal and VEGF-stimulated condition.[18] Thus, de novo protein synthesis is indispensable for the induction of vasohibin mRNA.

Posttranslational Processing, Secretion, and Biological Activity

To understand the posttranslational modification of vasohibin protein, vasohibin cDNA was overexpressed in ECs.[20] The calculated vasohibin protein is 44 kDa. When the retroviral vector encoding human vasohibin cDNA was transfected to the HUVEC-derived HUV-SV8 cells, 2 major (42, 36 kDa) bands and 2 minor (32, 27 kDa) bands were detected in their cellular extract, whereas 42 kDa product was detected in the conditioned medium. Because the 44 kDa complete from was not seen, amino terminal region is thought to be processed simultaneously or immediately after the translation. To characterize the structures of these multiple forms of vasohibin proteins, various vasohibin cDNA mutants were generated to substitute some basic amino acids. This analysis revealed that there were 2 cleaving sites in the amino terminal region; arginine 29 and arginine 76. The 42 kDa form is generated by the cleavage at arginine 29, whereas the 36 kDa form is generated by the cleavage at arginine 76. Because only 42 kDa vasohibin was shown in the conditioned medium, the domain from arginine 29 to arginine 76 is thought to be important for the secretion. The mechanism of its secretion is not known at present. Cleaving sites in the carboxyl terminal region are not determined yet. However, because the calculated molecular weight of the vasohibin protein from methionine 77 to carboxyl terminal end is 33 kDa, the carboxyl terminal of the 32 kDa form should be very close to the end. From the calculation of the molecular weight, the 27 kDa form may lack about 47 amino acids from the carboxyl-terminal, and this lacked region contains the cluster of basic amino acids (Figure 1).

To determine the biological function of these processed forms of vasohibin, mouse corneal miropocket assay was used to check for antiangiogenic activities using purified recombinant proteins for Vh(77–365) and Vh(77–318).[20] Vh(77–365) inhibited FGF-2–induced angiogenesis, suggesting that truncation of the 76 amino terminal residues does not influence antiangiogenic activity of vasohibin. On the other hand, Vh(77–318) could not exert antiangiogenic activity, suggesting that the carboxyl terminal is essential for antiangiogenic activity (Figure 1).

Application to Antiangiogenic Therapy

Because vasohibin is identified as a novel angiogenesis inhibitor, one may anticipate the application of vasohibin to antiangiogenic therapy. We have examined the effect of vasohibin on 3 different states of pathological angiogenesis: tumor angiogenesis, arterial adventitial angiogenesis, and retinal angiogenesis.

For tumor angiogenesis, we transfected human vasohibin cDNA into Lewis lung carcinoma (LLC) cells, establishing two permanent human vasohibin-producing clones.[16] Vasohibin cDNA transfection did not alter the proliferation of LLC cells in vitro. To show the effect of vasohibin produced by LLC cells on ECs, mock or vasohibin-transfected LLC cells were plated on the lower compartment of modified Boyden chambers, and the migration of HUVECs toward LLC cells was analyzed. The number of migrated HUVECs was significantly reduced when vasohibin-transfected LLC cells were plated on the lower chamber. Then LLC cells were inoculated intradermally in mice, and the growth of tumor was observed. The growth of vasohibin producing LLC cells in mice was significantly retarded, and immunohistological analysis of CD31 revealed that tumors of mock-transfectants contained large luminal vessels whereas those of vasohibin

producing LLC cells contained very small ones, even when the size of tumors did not differ dramatically.[16]

It has been documented that the extent of adventitial angiogenesis from vasa vasora correlates with atherosclerosis.[21] Arterial neointimal formation was investigated using the mouse cuff model.[22] In this model, cuff placement around the femoral artery does not denudate luminal endothelium, but induces adventitial angiogenesis, and that causes neointimal formation. To apply vasohibin protein to mice, we injected replication-defective adenovirus vectors encoding human vasohibin gene (AdVh) to mice via the tail vein. In this way, vasohibin was synthesized in the liver, secreted in the plasma, and was able to exhibit antiangiogenic activity in the remote sites after the delivery through systemic circulation.[22] We observed that adventitial angiogenesis and neointimal formation were significantly inhibited in AdVh-injected mice in this model. Thus, vasohibin is thought to play a preventive role in angiogenesis-dependent neointimal formation.

Retinal angiogenesis is the major cause of acquired blindness.[23] The mouse model of retinopathy of premature (ROP) is a useful model to study the hypoxia-induced regulation of VEGF expression.[24] In this model, placement of neonatal mice into a high oxygen environment results in decreased expression of VEGF and regression of newly developed retinal blood vessels. When mice are returned to room air, the poorly vascularized retina becomes hypoxic and VEGF is induced, which causes retinal angiogenesis. Interestingly, when endogenous vasohibin expression in the retinal vessels was knocked down by siRNA, retinal angiogenesis was augmented.[25] This result indicates that endogenous vasohibin plays a role in the inhibition of angiogenesis. However, it is assumed that the extent of endogenous vasohibin expression is not enough to control retinal angiogenesis. To determine the effect of exogenous vasohibin, we used AdVh or recombinant vasohibin protein. Intraocular injection of recombinant vasohibin or AdVh strongly suppressed retinal angiogenesis.[25]

A Homologue of Vasohibin and Splicing Variants

By the search of DNA sequences in the database, a homologous gene was found. This gene was named vasohibin-2, and the prototype vasohibin as renamed vasohibin-1.[17] Human vasohibin-2 is composed of 355 amino acid residues, and also exhibits antiangiogenic activity. The overall homology between human vasohibin-1 and vasohibin-2 is 52.5% at the amino acid level. The genes for human vasohibin-1 and vasohibin-2 are located on chromosome 14q24.3 and 1q32.3, respectively.

So far 8 exons for the vasohibin-1 gene and 11 exons for the vasohibin-2 gene have been shown in Ensembl human genome database to form multiple transcripts for these paralogous genes owing to alternative splicing (Figure 2). Prototype full-length vasohibin-1 is composed with 5589 bp consisting of 8 exons, and will receive posttranslational processing as described previously. In addition, two splicing variants of 522 bp and 1459 bp have been registered in the database. Although open reading frames encoding 42 and 204 amino acids, respectively, exists in these transcripts and the expression of all three splicing variants are confirmed by real-time polymerase chain reaction using unique primers (unpublished observation, 2006), the biological significance

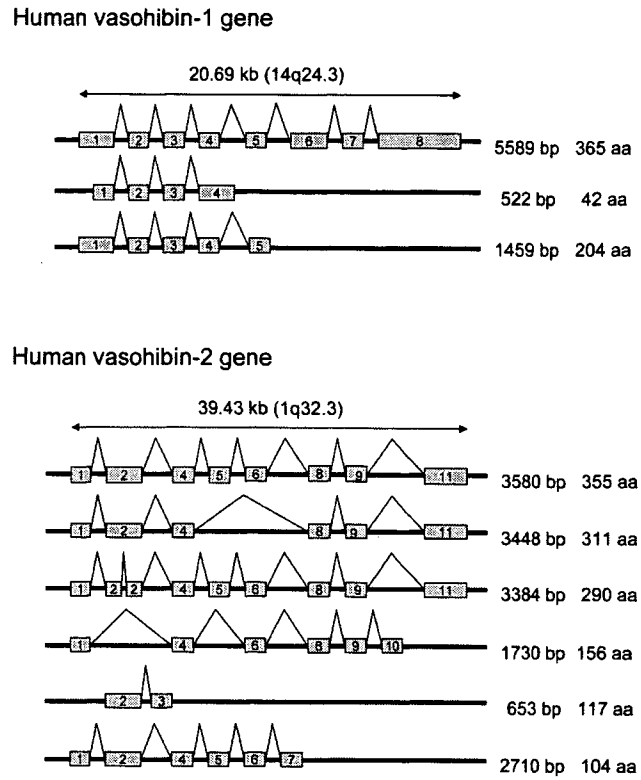

Figure 2. Schematic representation of human vasohibin-1 and -2 genomic structures and splicing patterns. Exons of human vasohibin-1 and vasohibin-2 genes are numbered in their orders on the chromosomes. Length of each transcript (bp) and polypeptides encoded in each transcript (aa) are shown in the right side of each splicing pattern.

of the 2 shorter variants have not been clarified yet. No alternative splicing for the mouse vasohibin-1 gene has been reported.

We have recently described the existence of 3 splicing variants for human vasohibin-2 transcripts, which encode polypeptides of 290, 311, and 355 amino acids.[17] Eight exons are joined to generate the variant of 355 amino acids, and this isoform is predominantly expressed in HUVECs. The isoform consisting of 290 amino acids has been confirmed to have antiangiogenic activity. In addition to those 8 exons, 3 additional exons are now found in Ensembl database generating 3 small different splicing variants encoding polypeptides of 104, 117, and 156 amino acids. The biological significance of these shorter variants have not been clarified yet. In the mouse genome, vasohibin-1 gene is located at 12D2 spanning 13.39 kb and consisting of 7 exons. Mouse vasohibin-2 gene is located at chromosome 1H6 spanning 31.48 kb and single splicing pattern with 8 exons is reported in Ensembl database.

Whereas the expression of vasohibin-2 was compared with that of vasohibin-1, vasohibin-2 expression in cultured endothelial cells was low and not inducible by the stimulation that induced vasohibin-1. However, the expression pattern of vasohibin-2 in vivo resembled to that of vasohibin-1.[17] Immunohistochemical analysis revealed that vasohibin-1 and vasohibin-2 were diffusely expressed in ECs in embryonic organs during midgestation. After that time point,

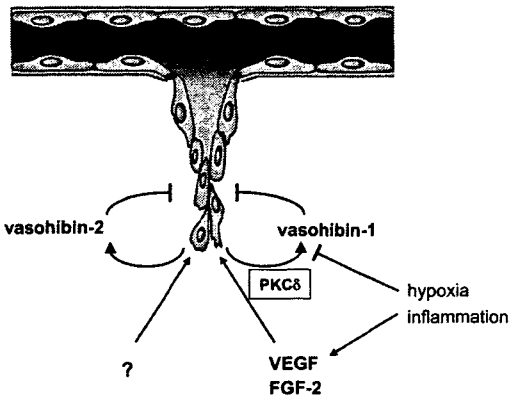

Figure 3. The role of vasohibin family in the regulation of angiogenesis. Vasohibin-1 and vasohibin-2 form a novel family of angiogenesis inhibitors genetically programmed in ECs. Vasohibin-1 is induced in ECs by VEGF and FGF-2. Hypoxia and inflammatory cytokines, which induce VEGF, may abort the expression of vasohibin-1 in ECs. The mechanism for the regulation of vasohibin-2 expression is not known.

vasohibin-1 and vasohibin-2 became faint, but persisted to a certain extent in arterial ECs from late-gestation to neonate. Interestingly, expression of vasohibin-1 and vasohibin-2 could be augmented in vivo by the local expression with the VEGF gene in the embryonic brain, or by cutaneous wounding in adult mice.[17]

Concluding Remarks

A summary of the vasohibin family is shown in Figure 3. Negative feedback regulation is one of the most important physiological mechanisms, and has been demonstrated to control a wide range of phenomena. However, very few endothelium-derived negative feedback regulators have been established for the regulation of angiogenesis. Vasohibin-1 is the first secretory antiangiogenic factor induced by VEGF in ECs. We would like to propose that vasohibin-1 has the property of negative feedback regulator of angiogenesis. Thus far Vasohibin-2 is a sole homologue of vasohibin-1, which exhibits antiangiogenic activity as well. Although vasohibin-2 lacks the property of VEGF or FGF-2 inducibility in vitro, its expression pattern is resemble to that of vasohibin-1. Thus, vasohibin-1 and vasohibin-2 form a novel family of angiogenesis inhibitors genetically programmed in ECs. The discovery of vasohibin family should shed light on the novel genomic basis of the negative regulation of angiogenesis.

Acknowledgments

We thank Dr Pieter Koolwijk at VU University Medical Center for valuable comments on this manuscript.

Disclosures

None.

References

1. Risau W. Mechanisms of angiogenesis. *Nature.* 1997;386:671–674.
2. Ferrara N. Vascular endothelial growth factor: basic science and clinical progress. *Endocr Rev.* 2004;25:581–611.
3. Eklund L, Olsen BR. Tie receptors and their angiopoietin ligands are context-dependent regulators of vascular remodeling. *Exp Cell Res.* 2006; 312:630–641.
4. Lee HJ, Cho CH, Hwang SJ, Choi HH, Kim KT, Ahn SY, Kim JH, Oh JL, Lee GM, Koh GY. Biological characterization of angiopoietin-3 and angiopoietin-4. *FASEB J.* 2004;18:1200–1208.
5. Sato Y. Update on endogenous inhibitors of angiogenesis. *Endothelium.* 2006;13:147–155.
6. Yamaguchi S, Iwata K, Shibuya M. Soluble Flt-1 (soluble VEGFR-1), a potent natural antiangiogenic molecule in mammals, is phylogenetically conserved in avians. *Biochem Biophys Res Commun.* 2002;291:554–559.
7. Zhai Y, Ni J, Jiang GW, Lu J, Xing L, Lincoln C, Carter KC, Janat F, Kozak D, Xu S, Rojas L, Aggarwal BB, Ruben S, Li LY, Gentz R, Yu GL. VEGI, a novel cytokine of the tumor necrosis factor family, is an angiogenesis inhibitor that suppresses the growth of colon carcinomas in vivo. *FASEB J.* 1999;13:181–189.
8. Haridas V, Shrivastava A, Su J, Yu GL, Ni J, Liu D, Chen SF, Ni Y, Ruben SM, Gentz R, Aggarwal BB. VEGI, a new member of the TNF family activates nuclear factor-kappa B and c-Jun N-terminal kinase and modulates cell growth. *Oncogene.* 1999;18:6496–6504.
9. Xiao Q, Hsu CY, Chen H, Ma X, Xu J, Lee JM. Characterization of cis-regulatory elements of the vascular endothelial growth inhibitor gene promoter. *Biochem J.* 2005;388:913–920.
10. Abe M, Sato Y. cDNA microarray analysis of the gene expression profile of VEGF-activated human umbilical vein endothelial cells. *Angiogenesis.* 2001;4:289–298.
11. Fuentes JJ, Genesca L, Kingsbury TJ, Cunningham KW, Perez-Riba M, Estivill X, de la Luna S. DSCR1, overexpressed in Down syndrome, is an inhibitor of calcineurin-mediated signaling pathways. *Hum Mol Genet.* 2000;9:1681–1690.
12. Yao YG, Duh EJ. VEGF selectively induces Down syndrome critical region 1 gene expression in endothelial cells: a mechanism for feedback regulation of angiogenesis? *Biochem Biophys Res Commun.* 2004;321:648–656.
13. Minami T, Horiuchi K, Miura M, Abid MR, Takabe W, Noguchi N, Kohro T, Ge X, Aburatani H, Hamakubo T, Kodama T, Aird WC. Vascular endothelial growth factor- and thrombin-induced termination factor, Down syndrome critical region-1, attenuates endothelial cell proliferation and angiogenesis. *J Biol Chem.* 2004;279:50537–50554.
14. Iizuka M, Abe M, Shiiba K, Sasaki I, Sato Y. Down syndrome candidate region 1 (DSCR1), a downstream target of VEGF in endothelial cells, regulates cell migration and angiogenesis via the functional interaction with integrin $\alpha v\beta 3$. *J Vasc Res.* 2004;41:334–344.
15. Cho Y-J, Abe M, Kim SY, Sato Y. Raf-1 is a binding partner of DSCR1. *Arch Biochem Biophys.* 2005;439:121–128.
16. Watanabe K, Hasegawa Y, Yamashita H, Shimizu K, Ding Y, Abe M, Ohta H, Imagawa K, Hojo K, Maki H, Sonoda H, Sato Y. Vasohibin as an endothelium-derived negative feedback regulator of angiogenesis *J Clin Invest.* 2004;114:898–907.
17. Shibuya T, Watanabe K, Yamashita H, Shimizu K, Miyashita H, Abe M, Moriya T, Ohta H, Sonoda H, Shimosegawa T, Tabayashi K, Sato Y. Isolation of vasohibin-2 as a sole homologue of VEGF-inducible endothelium-derived angiogenesis inhibitor vasohibin: a comparative study on their expressions. *Arterioscl Thromb Vasc Biol.* 2006;26:1051–1057.
18. Shimizu K, Watanabe K, Yamashita H, Abe M. Yoshimatsu H, Ohta H, Sonoda H, Sato Y. Gene regulation of a novel angiogenesis inhibitor, vasohibin, in endothelial cells. *Biochem Biophys Res Commun.* 2005;327:700–706.
19. Harrington EO, Loffler J, Nelson PR, Kent KC, Simons M, Ware JA. Enhancement of migration by protein kinase Calpha and inhibition of proliferation and cell cycle progression by protein kinase Cdelta in capillary endothelial cells. *J Biol Chem.* 1997;272:7390–7397.
20. Sonoda H, Ohta H, Watanabe K, Yamashita H, Kimura H, Sato Y. Multiple processing forms and their biological activities of a novel angiogenesis inhibitor vasohibin. *Biochem Biophys Res Commun.* 2006;342:640–646.
21. Fleiner M, Kummer M, Mirlacher M, Sauter G, Cathomas G, Krapf R, Biedermann BC. Arterial neovascularization and inflammation in vulnerable patients: early and late signs of symptomatic atherosclerosis. *Circulation.* 2004;110:2843–2850.
22. Yamashita H, Abe M, Watanabe K, Shimizu K, Moriya T, Sato A, Satomi S, Ohta H, Sonoda H, Sato Y. Vasohibin prevents arterial neointimal formation through angiogenesis inhibition. *Biochem Biophys Res Commun.* 2006;345:919–925.
23. Campochiaro PA. Ocular neovascularisation and excessive vascular permeability. *Expert Opin Biol Ther.* 2004;4:1395–1402.
24. Campochiaro PA, Hackett SF. Ocular neovascularization: a valuable model system. *Oncogene.* 2003;22:6537–6548.
25. Shen JK, Yang XR, Sato Y, and Campochiaro PA. Vasohibin is Up-regulated by VEGF in the Retina and Suppresses VEGF receptor 2 and Retinal Neovascularization. *FASEB J.* 2006;20:723–725.

The EMBO Journal (2008) 27, 522–534 | © 2008 European Molecular Biology Organization | All Rights Reserved 0261-4189/08
www.embojournal.org

THE EMBO JOURNAL

Spatial and temporal role of the apelin/APJ system in the caliber size regulation of blood vessels during angiogenesis

Hiroyasu Kidoya[1], Masaya Ueno[1], Yoshihiro Yamada[1], Naoki Mochizuki[2], Mitsugu Nakata[3], Takashi Yano[3], Ryo Fujii[4] and Nobuyuki Takakura[1,*]

[1]Department of Signal Transduction, Research Institute for Microbial Diseases, Osaka University, Suita, Osaka, Japan, [2]Department of Structural Analysis, National Cardiovascular Center Research Institute, Suita, Osaka, Japan, [3]Pharmaceutical Research Laboratories 1, Pharmaceutical Research Division, Takeda Pharmaceutical Company Limited, Yodogawa, Osaka, Japan and [4]Frontier Research Laboratories, Pharmaceutical Research Division, Takeda Pharmaceutical Company Limited, Tsukuba-shi, Ibaraki, Japan

Blood vessels change their caliber to adapt to the demands of tissues or organs for oxygen and nutrients. This event is mainly organized at the capillary level and requires a size-sensing mechanism. However, the molecular regulatory mechanism involved in caliber size modification in blood vessels is not clear. Here we show that apelin, a protein secreted from endothelial cells under the activation of Tie2 receptor tyrosine kinase on endothelial cells, plays a role in the regulation of caliber size of blood vessel through its cognate receptor APJ, which is expressed on endothelial cells. During early embryogenesis, APJ is expressed on endothelial cells of the new blood vessels sprouted from the dorsal aorta, but not on pre-existing endothelial cells of the dorsal aorta. Apelin-deficient mice showed narrow blood vessels in intersomitic vessels during embryogenesis. Apelin enhanced endothelial cell proliferation in the presence of vascular endothelial growth factor and promoted cell-to-cell aggregation. These results indicated that the apelin/APJ system is involved in the regulation of blood vessel diameter during angiogenesis.

The EMBO Journal (2008) **27**, 522–534. doi:10.1038/sj.emboj.7601982; Published online 17 January 2008
Subject Categories: development
Keywords: angiogenesis; angiopoietin-1; apelin; APJ; lumen size

Introduction

The vascular system of vertebrates has a highly organized and hierarchical structure, ranging from large blood vessels down to finely sized capillaries. The intraluminal cavity of blood vessels is lined almost exclusively with endothelial cells (ECs). The formation of blood vessels is initiated by the assembly and tube formation of ECs, or EC progenitors. This process is termed vasculogenesis and is followed by angiogenesis, which results in the emergence of new vessels through sprouting and elongation from, or the remodelling of, pre-existing vessels (Risau, 1997).

Many genes involved in these processes have been isolated and their roles in the specification of vascular lineage from mesodermal cells and vascular morphogenesis have been analysed (Wang *et al*, 1998; Adams *et al*, 1999; Gale and Yancopoulos, 1999; Oettgen, 2001; Zhong *et al*, 2001; Carmeliet, 2003; Gerhardt and Betsholtz, 2003; Simon, 2004). Among many molecules, vascular endothelial growth factors (VEGFs) and their cognate receptors (VEGFRs) play central roles in the differentiation (arterial), proliferation, migration and survival of ECs in physiological and pathological conditions (Ferrara *et al*, 2003). Based on the diverse functions of VEGFs in blood vessel formation, the VEGF/VEGFR system has proved effective in the clinical management of cancer patients by negatively regulating angiogenesis (Ferrara and Alitalo, 1999; Jain, 2005). Therefore, these results indicate the importance of developmental studies for understanding blood vessel formation.

In the maturation process involved in blood vessel formation, the ECs, which form the tube, recruit supporting mural cells (MCs) such as periendothelial cells (pericytes) or vascular smooth muscle cells, by releasing platelet-derived growth factor (PDGF)-BB (Lindahl *et al*, 1997). MCs subsequently adhere to ECs resulting in the formation of a structurally stable blood vessel. It has been proposed that this cell adhesion between ECs and MCs is induced when angiopoietin 1 (Angl), produced from MCs, stimulates Tie2, a receptor tyrosine kinase on ECs (Dumont *et al*, 1994; Sato *et al*, 1995; Suri *et al*, 1996).

During angiogenesis, blood vessels need to be able to adjust their caliber, in order to allow them to respond adequately to the changes in demand for oxygen and nutrients made by the organs and tissues. This caliber adjustment is involved in the maturation process during angiogenesis; however, the molecular mechanism involved in the determination of blood vessel size has not been elucidated. A potent regulator of the enlargement of blood vessel caliber is the Angl/Tie2 system, because transgenic overexpression of Angl in the keratinocyte-induced enlarged blood vessels in the dermis (Suri *et al*, 1998) and administration of a potent Angl variant were also reported to induce enlargement of blood vessels (Cho *et al*, 2005; Thurston *et al*, 2005). Therefore, the analysis of the precise molecular mechanism of how the Angl/Tie2 system induces enlargement of blood vessels would allow us to understand the process of determination of blood vessel size during angiogenesis.

In this report, by the analysis of downstream signalling of Angl/Tie2 in ECs, we found that apelin, a recently isolated bioactive peptide from bovine gastric extract working as a

*Corresponding author. Department of Signal Transduction, Research Institute for Microbial Diseases, Osaka University, 3-1 Yamadaoka, Suita, Osaka 565-0871, Japan. Tel.: +81 6 6879 8316; Fax: +81 6 6879 8314; E-mail: ntakaku@biken.osaka-u.ac.jp

Received: 19 April 2007; accepted: 18 December 2007; published online: 17 January 2008

ligand for APJ, is upregulated by Ang1 stimulation of human umbilical vein endothelial cells (HUVECs). A sequence of apelin cDNA encodes a protein of 77 amino acids, which can generate two active polypeptides: the long (42–77) and the short (65–77) forms of apelin (Tatemoto *et al*, 1998; Kawamata *et al*, 2001; Masri *et al*, 2005). Both forms activate APJ.

APJ is a G protein-coupled receptor, which has been reported to be expressed in the cardiovascular and central nervous systems (O'Dowd *et al*, 1993; Devic *et al*, 1999). In brain tissues, APJ expression is observed in neurons (Edinger *et al*, 1998) as well as in oligodendrocytes and astrocytes (Croitoru-Lamoury *et al*, 2003). In the brain, the apelin/APJ system plays a role in maintaining body fluid homeostasis and regulating the release of vasopressin from the hypothalamus (De Mota *et al*, 2004). In the cardiovascular system, APJ is expressed in an endothelial lineage in various species such as amphibian, mouse and human (Devic *et al*, 1996, 1999; Katugampola *et al*, 2001). In the mouse and human, the expression of the receptor has also been detected by immunocytochemistry in vascular smooth muscle cells and cardiomyocytes (Kleinz and Davenport, 2004). Apelin/APJ function in cardiomyocytes is thought to be associated with a very strong inotropic activity (Szokodi *et al*, 2002; Ashley *et al*, 2005). The function of apelin/APJ in EC lineage is reported to be associated with the hypotensive activity of apelin (Ishida *et al*, 2004), as the activation of APJ leads to nitric oxide (NO) production by the ECs (Tatemoto *et al*, 2001), and this possibly plays a role in the relaxation of smooth muscle cells.

Using the morpholino antisense oligonucleotide, requisite roles of the apelin/APJ system have been reported in the cardiovascular system of *Xenopus laevis* (Cox *et al*, 2006; Inui *et al*, 2006) and zebrafish (Scott *et al*, 2007). *Xenopus apelin* (*Xapelin*) was detected in the region around the presumptive blood vessels during early embryogenesis and overlapped with the expression of *Xmsr*, the *Xenopus* homolog of *APJ*. Overexpression of *Xapelin* disorganized the expression of the endothelial precursor cell marker *XlFli* at the neurula stage. Knockdown of *Xapelin* or Xmsr induced abnormal heart morphology and attenuated the expression of *Tie2*, resulting in the disruption of blood vessel formation in the posterior cardinal vein, intersomitic vessels (ISVs) and vitelline vessels. By contrast, apelin protein has been shown to induce angiogenesis in the chicken chorioallantoic membrane assay (Cox *et al*, 2006). Although the involvement of apelin/APJ in angiogenesis and the regulation of proliferation of ECs has been suggested, the precise function of apelin/APJ in the morphology of blood vessels in mammals is not clear.

Here, using various *in vitro* and *in vivo* assays, we show that apelin induces enlargement of blood vessels. Moreover, the physiological function of apelin has been studied through the generation of apelin-mutant mice and the relationship of Ang1/Tie2 signalling to apelin has been studied by mating apelin-mutant mice with Ang1 transgenic mice. Finally, using the para-aortic splanchnopleural mesoderm (P-Sp) organ culture system that mimics *in vivo* vasculogenesis and angiogenesis and various *in vitro* HUVEC culture systems, we have studied how apelin regulates the enlargement of blood vessels.

Results

Ang1 induces apelin expression on ECs

To elucidate the molecular mechanism by which Tie2 regulates the caliber change of blood vessels from small to larger ones, and in order to isolate the genes encoding proteins that are involved in caliber change and specifically expressed in HUVECs stimulated by Ang1, we constructed a subtraction library from HUVECs with Tie2 stimulated by Ang1 as a tester, and HUVECs with no stimulation of Tie2 as the driver (Figure 1A). One of these isolated cDNA clones was the human gene encoding apelin (Figure 1B–D). Real-time polymerase chain reaction (PCR) analysis revealed that apelin mRNA was potently increased in HUVECs after stimulation by Ang1 in a time-dependent manner (Figure 1B) and we confirmed that the expression of apelin protein was markedly upregulated on HUVECs stimulated by Ang1 (Figure 1C). Moreover, the dose-dependent effect of Ang1 on apelin production from HUVECs was confirmed by enzyme immunoassay, using the culture supernatant of HUVECs (Figure 1D).

In order to confirm further the upregulation of apelin in ECs *in vivo*, we analysed apelin expression in the dermis of Ang1 transgenic (Ang1Tg) mice, in which Ang1 was overexpressed in the keratinocytes under the transcriptional control of K14 promoter (Suri *et al*, 1998). As shown in Figure 1E, apelin expression on ECs in the dermis at postnatal day 7 was increased in Ang1Tg mice compared to that in wild-type (WT) mice. We confirmed the overexpression of apelin mRNA in Ang1Tg mice by quantitative real-time RT–PCR using ECs fractionated from the dermis by a cell sorter (Figure 1F). As it is well known that Ang1 is involved in angiogenesis, next we observed the effect of other proangiogenic molecules on the expression of apelin on ECs. bFGF induced apelin expression on HUVECs; however, VEGF, PDGF-BB or EGF did not affect apelin expression (Supplementary Figure 1A and B).

Apelin with VEGF induces proliferation of ECs

With respect to the enlargement of blood vessels, it seems likely that apelin causes the proliferation of ECs. To test this ability, firstly we studied the proliferation of ECs using HUVECs. As shown in Figure 2A, apelin was not effective in inducing proliferation of HUVECs. However, upon stimulation with VEGF, the expression level of APJ was upregulated in HUVECs, at both the mRNA and protein levels (Figure 2B–D and Supplementary Figure 2). Cell surface expression of APJ on HUVECs was confirmed by both cell surface biotinylation experiment (Figure 2D) and confocal laser scanning analysis (Supplementary Figure 2). Consistent with this result, VEGF-induced proliferation of HUVECs was enhanced by the addition of apelin in a dose-dependent manner (Figure 2A). Among proangiogenic cytokines, such as Ang1, EGF, bFGF, PDGF-BB and VEGF, only VEGF induced APJ expression on HUVECs (Figure 2B–D and Supplementary Figure 1C and D).

These results suggested that APJ is expressed and affects ECs during angiogenesis in which VEGF levels are upregulated. Next we observed the proliferation of primary ECs from the culture of the AGM region (aorta–gonad–mesonephros region followed by P-Sp region at embryonic day (E) 10.5 to E11.5) in which angiogenesis was actively taking place. APJ was highly expressed in the AGM region compared to other tissues, such as E10.5 yolk sac, head region and heart, and adult heart (Figure 3A). Furthermore, APJ was expressed strongly in $CD45^{-}CD31^{+}$ ECs from the AGM region compared to those from E10.5 heart and adult heart. Although ECs in E10.5 yolk sac and head region expressed APJ, the

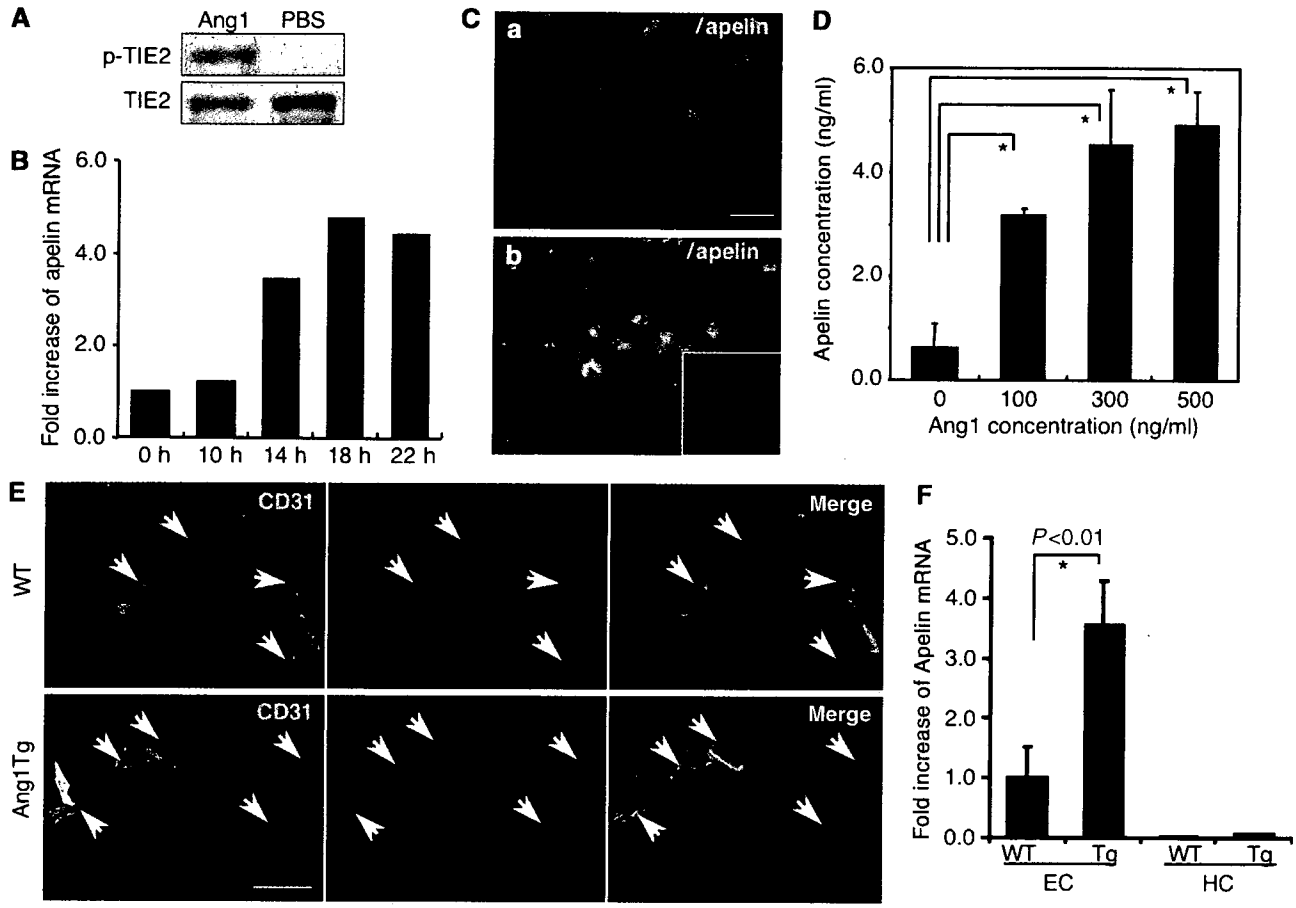

Figure 1 Ang1 stimulation induces apelin expression in ECs *in vitro* and *in vivo*. (**A**) Tie2 phosphorylation on HUVECs by Ang1 in our system. HUVECs, serum-starved for 2 h, were either treated or not treated with 500 ng/ml Ang1 for 10 min. Phosphorylation was studied by immunoblotting using phosphospecific antibody (p-Tie2). (**B**) Quantitative real-time RT–PCR analysis of apelin mRNA in HUVECs. Total RNA was extracted from HUVECs that had been stimulated with Ang1 for 0–22 h. Results are shown as fold increase in comparison with basal levels of HUVECs (0 h). (**C**) Immunocytochemical analysis of apelin expression in HUVECs, non-stimulated (a) and stimulated (b) by Ang1 (500 ng/ml) for 20 h. Cells were stained with anti-apelin mAb (green). The inset in (b) shows HUVECs stained with secondary antibody as a negative control. Nuclei were stained with propidium iodide (PI; red). Scale bar indicates 50 μm. (**D**) Quantitative enzyme immunoassay of apelin production from HUVECs stimulated by various doses of Ang1. $^*P<0.001$ ($n=3$). (**E**) Immunochemical detection of apelin peptide in the dermis. Sections of skin from WT and Ang1Tg neonatal mice were stained with anti-CD31 (green) and anti-apelin (red) mAb. Arrows indicate CD31$^+$ blood vessels. Scale bar indicates 30 μm. (**F**) Quantitative real-time RT–PCR analysis of apelin mRNA in ECs and hematopoietic cells (HCs) of Ang1Tg mice. RNA was prepared from sorted CD31$^+$CD45$^-$ ECs or CD31$^-$CD45$^+$ HCs from the dermis of WT or Ang1Tg neonatal mouse skin. $^*P<0.01$ ($n=3$).

expression level was weaker than that in the AGM region. When cells from the AGM region were cultured on apelin-expressing OP9 cells (Figure 3B), proliferation of CD45$^-$CD31$^+$ was increased compared with that on control OP9 cells and this proliferation by apelin was abrogated by the addition of anti-apelin blocking antibody (Figure 3C and D), suggesting that this action of proliferation by apelin is specific to the apelin/APJ system. Moreover, as APJ expression was weaker in ECs from adult heart (Figure 3A) or adult liver (data not shown) than in those from the AGM region, apelin did not induce proliferation of ECs in such adult tissues compared to those in the AGM region (Supplementary Figure 3).

Apelin induces the assembly of ECs

Although the proliferation of ECs is one of the factors involved in the construction of larger vessels, it is not the only one. The assembly or aggregation of ECs or endothelial progenitors, resulting in abundant cell-to-cell contact, is also necessary for the induction of a caliber change of blood vessels into larger ones. Therefore, next we tested the ability of apelin to regulate cell-to-cell contact. When cells from the AGM region were put on OP9 feeder cells, the control OP9 cells induced a cord-like structure of ECs, in contrast to the OP9 cells expressing apelin, which induced a sheet-like layer of ECs in abundance (Figure 4A and C). When cell-to-cell contact was observed using anti-VE-cadherin or -claudin5 antibodies, we confirmed that the sheet-like structure was composed of ECs connected with the junctional proteins, VE-cadherin (Figure 4B) or claudin5 (Supplementary Figure 4). Moreover, the addition of anti-apelin monoclonal antibody (mAb) inhibited the sheet-like layer formation of ECs induced by apelin (Figure 4B and Supplementary Figure 4). This sheet-like structure was already observed in the early stage of this culture (Figure 4C), suggesting that cell aggregation was initiated when ECs were seeded on OP9 cells expressing apelin.

Among many adhesion molecules tested, we found that the expression of the junctional protein, claudin5, was significantly induced by apelin on HUVECs, while that of VE-cadherin was only slightly induced, at both the mRNA

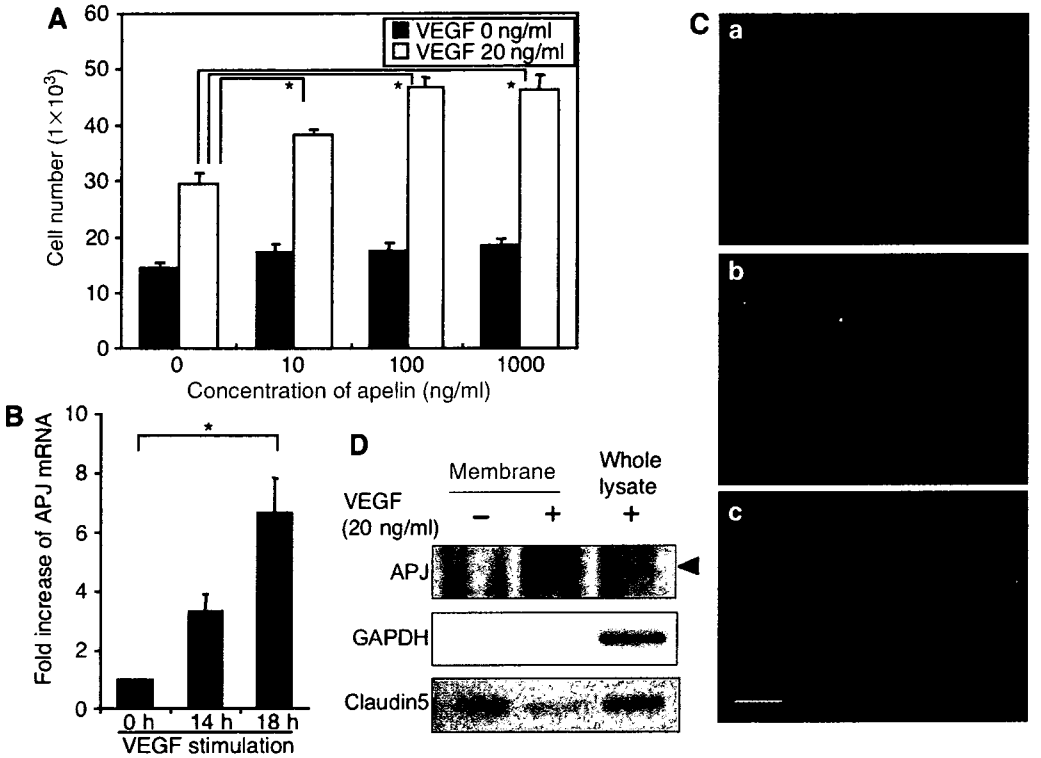

Figure 2 Apelin induces proliferation of HUVECs in a VEGF-dependent manner. (**A**) Proliferation of HUVECs by apelin. HUVECs (5×10^3) were cultured with apelin (0–1000 ng/ml) in the presence or absence of VEGF (20 ng/ml) for 48 h and the number of cells was counted. $^*P<0.001$ ($n=3$). (**B**) Quantitative real-time RT–PCR analysis of the induction of APJ expression by VEGF in HUVECs. HUVECs were stimulated with VEGF (10 ng/ml) for 0–18 h. Results are shown as fold increase in expression in comparison with levels in stimulated HUVECs at 0 h. $^*P<0.001$ ($n=3$). (**C**) APJ expression on HUVECs. HUVECs were cultured in the absence (a) or presence (b, c) of VEGF (20 ng/ml) for 24 h and stained with anti-APJ antibody (green) (a, b). (c) Cells stained with a secondary antibody alone as a negative control. Nuclei were stained with propidium iodide (red). Scale bar indicates 50 μm. (**D**) Western blot analysis of cell surface APJ expression on HUVECs that had been stimulated with VEGF (20 ng/ml) for 24 h. The purity of cell membrane protein was confirmed by the lack of intracellular protein GAPDH expression. Claudin5 expression was analysed for the experimental control of another cell surface protein. Note that the expression of a 60 kDa APJ protein was increased in HUVECs in the presence of VEGF.

and protein levels (Supplementary Figure 5). *In vitro* sheet-like formation of ECs and upregulation of cell-to-cell adhesion molecules by apelin indicated the involvement of the apelin/APJ system in the assembly of ECs. Next, we performed the cord formation assay of HUVECs on Matrigel in the presence or absence of apelin (Figure 5A). After 20 h of culture of HUVECs on Matrigel, they formed a cord-like structure in the absence of apelin (Figure 5Aa). However, in the presence of apelin, the HUVECs formed an enlarged cord-like structure (Figure 5Abd). In this assay, by using confocal laser scanning analysis, we confirmed that enlargement of this cord-like structure was induced by cell aggregation, but not by cell spreading (Supplementary Figure 6). This enlargement was completely blocked by anti-VE-cadherin blocking antibody (Figure 5Acd), suggesting that the enlarged cord-like formation induced by apelin was initiated by cell-to-cell contact. Moreover, in the spheroid assay (Korff and Augustin, 1998), HUVECs formed large spheroids in the presence of apelin (Figure 5B) and this action was abrogated by anti-apelin antibody. Therefore, these results strongly support the notion that the apelin/APJ system induces EC-to-EC assembly.

APJ expression in ECs during early embryogenesis

As APJ expression was observed in ECs during early embryogenesis (Figure 3), we studied which vessels expressed APJ in mouse embryos. At E8.5, cells committed into the endothelial lineage formed the dorsal aorta (DA), from which ECs started to sprout. As observed in Figure 6A, APJ expression was observed in those ECs that had sprouted from the DA but not in those that were forming the DA. At E9.5, APJ expression was observed in the migrating end region of ISVs sprouting from the DA (Figure 6B). Besides the expression of APJ in the ISVs, weak APJ expression was observed in the somites. These expression profiles were not very different from the results obtained by *in situ* hybridization analysis, as reported previously (Devic *et al*, 1999). In another area of the E9.5 embryo, we found that the anterior cardinal vein (ACV) expressed APJ. However, when compared to CD31 expression in ECs, APJ-positive ECs were observed in the migrating end of the ACV, but not in the base (Supplementary Figure 7). These expression profiles suggest that the apelin/APJ system may be associated with angiogenesis but not with vasculogenesis. Moreover, when apelin expression was observed in the somite region at E9.5, we found that apelin protein was detected in ISV (Supplementary Figure 8), suggesting that the apelin/APJ system may be associated with the formation of ISV.

Narrow blood vessels are induced in apelin-mutant mice

In order to understand the physiological function of apelin, we generated apelin-mutant mice (Supplementary Figure 9)

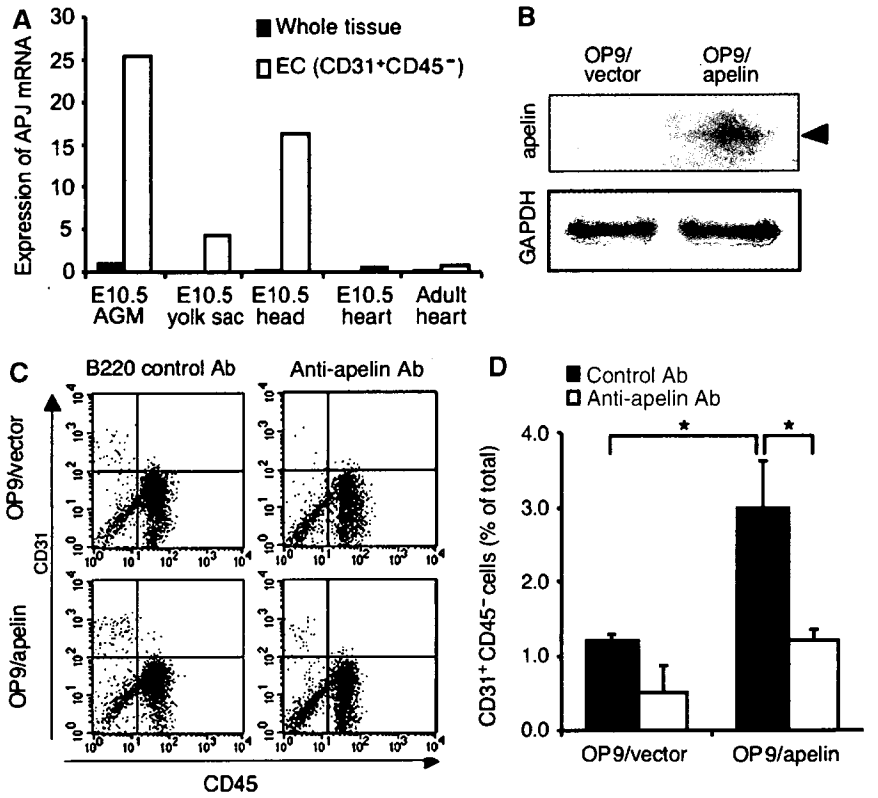

Figure 3 ECs from the AGM region express APJ and are induced to proliferate by apelin. (**A**) Quantitative real-time RT–PCR analysis of APJ expression in various tissues, as indicated. RNA from whole tissue, or $CD45^{-}CD31^{+}$ ECs sorted from various tissues, was evaluated for the expression of APJ. (**B**) Western blot analysis of apelin expression on OP9 cells induced by mock vector (OP9/vector) or apelin expression vector (OP9/apelin). An 8 kDa apelin protein was detected in OP9/apelin. GAPDH was used for the internal control. (**C**) Apelin-induced proliferation of ECs from E10.5 AGM region. Cells from the AGM region were cultured for 7 days, on an OP9/vector or OP9/apelin, in the presence or absence of anti-apelin or control B220 mAb. AGM cells harvested from cultures were stained with anti-CD31 and -CD45 mAbs and analysed by FACS. (**D**) Quantitative evaluation of the percentage of $CD31^{+}CD45^{-}$ vascular ECs cultured as described in (C). $^{*}P<0.001$ ($n=5$).

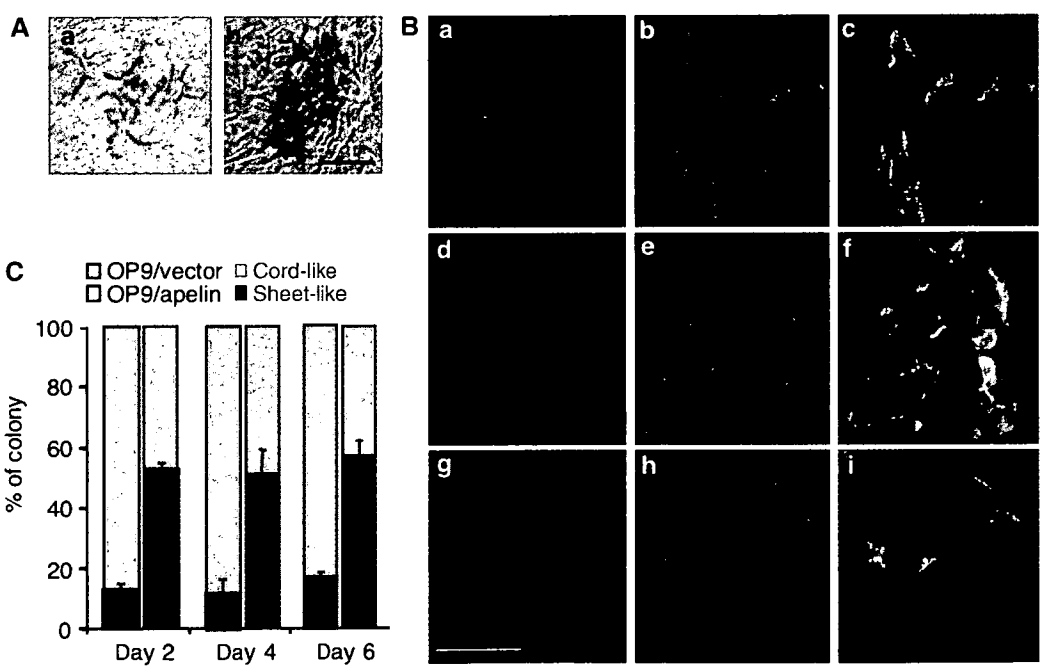

Figure 4 Endothelial sheet formation by apelin. (**A**) Cells from E11.5 AGM region were cocultured with an OP9/vector (a) or OP9/apelin (b) for 2–6 days, and CD31 immunostaining was performed. The arrow indicates the aggregated EC sheet. Scale bar indicates 100 μm. (**B**) Cells from E11.5 AGM region were cocultured for 6 days with an OP9/vector (a–c), OP9/apelin in the presence of B220 control antibody (d–f) or OP9/apelin in the presence of anti-apelin blocking antibody (g–i). ECs on OP9 cells were stained with anti-CD31 (a, d, g) and anti-VE-cadherin (b, e, h) antibodies. (c, f, i) Merged images of (a) and (b), (d) and (e), or (g) and (h), respectively. Scale bar indicates 50 μm. (**C**) The proportion of sheet-like or cord-like structures of ECs on OP9/apelin or OP9/vector stromal cells ($n=3$).

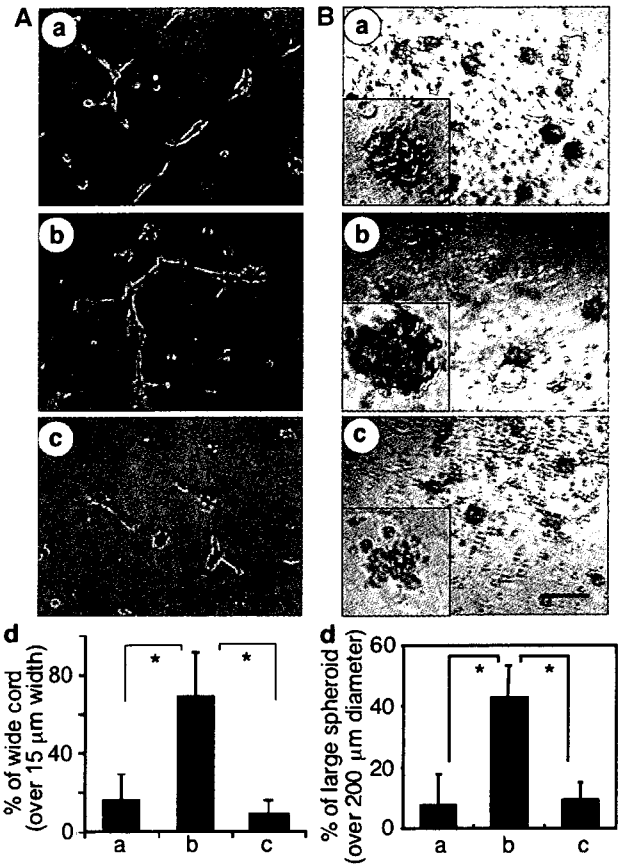

Figure 5 Morphological change of HUVECs stimulated with apelin. (**A**) Cord formation analysis of HUVECs cultured on Matrigel. HUVECs were cultured in the presence of VEGF (20 ng/ml) for 20 h, harvested, transferred onto Matrigel and cultured in the absence (a) or presence of apelin (b, c) for 10 h. Anti-VE-cadherin antibody (c) or control anti-B220 mAb (b) was added. Scale bar indicates 200 μm. (d) Quantitative evaluation of the width of the cord-like structure observed in the various culture conditions (a: control; b: apelin + anti-B220 mAb; c: apelin + anti- VE-cadherin antibody) described above. The percentage of wide cord (width >15 μm) among the total cord-like structure was calculated. *$P<0.01$ ($n=3$). (**B**) HUVEC spheroid assay. HUVECs stimulated with VEGF for 24 h were harvested and cultured on nonadhesive dishes in the absence (a) or presence of apelin (b, c) for 10 h. Anti-apelin antibody (c) or control anti-B220 mAb (b) was added. Scale bar indicates 500 μm. The inset in each panel shows higher magnified representative spheroid under each condition. (d) Quantitative evaluation of the size of spheroid observed in the various culture conditions (a: control; b: apelin; c: apelin + anti-apelin antibody) described above. The percentage of large spheroid (diameter >200 μm) among the total spheroid was calculated. *$P<0.01$ ($n=3$).

and observed blood vessel formation. Mice heterozygous for apelin were intercrossed and their offspring were obtained. The frequency of mutant homozygotes obtained in heterozygote intercrosses was close to the expected 25%, suggesting that apelin-deficient mice are not embryonically lethal. Although a small population of apelin-mutant mice lacked eyes and lost a great deal of weight, for reasons that have not been determined as yet, generally, the mutant animals appeared healthy as adults. Crosses between homozygous apelin-mutant animals were also fertile, indicating that implantation and embryonic development can apparently occur normally even when apelin is absent from both the embryo and the mother.

As apelin deficiency in *Xenopus* leads to severe disorganized blood vessel formation (Cox *et al*, 2006; Inui *et al*, 2006) and might induce embryonic lethality, it is possible that other unknown molecules compensate and rescue apelin deficiency in mammals. Before a compensatory effect was investigated, we studied the ISV at E9.5 (Figure 7A–C and Supplementary Figure 10), because we found that APJ expression was clearly observed in vessels sprouted from the DA into the somite (Figure 6). The results showed that body size and number of somites were equivalent between WT and apelin-mutant embryos at E9.5, but that the caliber of ISVs was narrower in apelin-deficient embryos compared with WT embryos. The expression of APJ was observed in all ECs of ISV sprouted from the DA, ranging from the base region of the sprout to the migrating end at E8.5; the expression had disappeared in the base region near the DA at E9.5 (Figure 6). This expression pattern in the phenotype of apelin-deficient embryos suggests that APJ expression is regulated by VEGF or other unknown molecules in ECs at the migrating end, in order to regulate the caliber size of blood vessels.

General Angl administration has been reported to induce enhancement of blood vessel formation in the trachea of adult mice (Cho *et al*, 2005). This indicates that tracheal blood vessels are active in angiogenesis in adulthood and it is possible that apelin deficiency affects blood vessel formation in this region. As expected, the blood vessels observed in the trachea of apelin-deficient mice were narrower than those in WT mice and, in addition, the capillary density was lower (Figure 8). Moreover, the blood vessels observed in the dermis (Figure 9 and Supplementary Figure 11) and heart (data not shown) of apelin-deficient mice were narrower than those in WT mice.

Through the use of the *in situ* hybridization method of APJ expression, it has been reported that APJ is not expressed on larger vessels such as DA, except for the posterior cardinal vein during early embryogenesis at around E9.5 (Devic *et al*, 1999). This result is consistent with our immunohistochemical analysis. The caliber sizes of the aorta and vena cava, and their major branches such as brachiocephalic, subclavian and common iliac arteries and veins, were not affected by the lack of apelin (data not shown). Therefore, this suggests that apelin may not be involved in the regulation of caliber size of larger vessels. Moreover, although apelin deficiency in *Xenopus* led to severely disorganized blood vessels in the vitelline (Cox *et al*, 2006; Inui *et al*, 2006), it did not affect the remodelling of blood vessels in the yolk sac (Supplementary Figure 12).

In order to analyse precisely the function of the exogenous apelin in the *in vitro* culture system, it was necessary to exclude from the analysis any confounding effects of the contaminating apelin from the culture serum, as well as the endogenous apelin produced from cultured cells. In order to achieve this, we tried to culture the aorta ring from apelin-deficient mice under quite low serum-containing conditions (Figure 7D and E). Although VEGF induced sprouting of ECs from the aorta, apelin on its own did not. However, the caliber size of VEGF-induced sprouts was enlarged upon the addition of apelin. Most of the sprouts induced by VEGF plus apelin contained large luminal cavities (data not shown). Therefore, we confirmed that apelin regulates caliber change in angiogenesis and this effect is induced in the

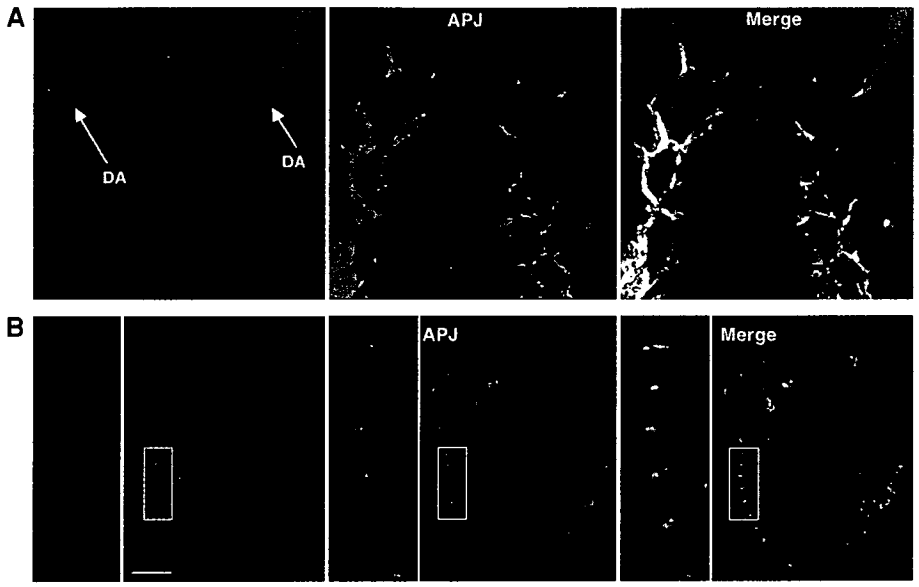

Figure 6 Expression of APJ in embryo. (**A**) Whole-mount staining of E8.5 mouse embryo with anti-CD31 (red) and anti-APJ (green) antibodies. (**B**) Staining of E9.5 mouse embryo section with anti-CD31 (red) and anti-APJ (green) Abs. The left panel shows high-power view of the area indicated by the box. Note that the DA stained by anti-CD31 Ab did not express APJ and APJ expressed on ECs sprouting from DA. Scale bar indicates 500 μm.

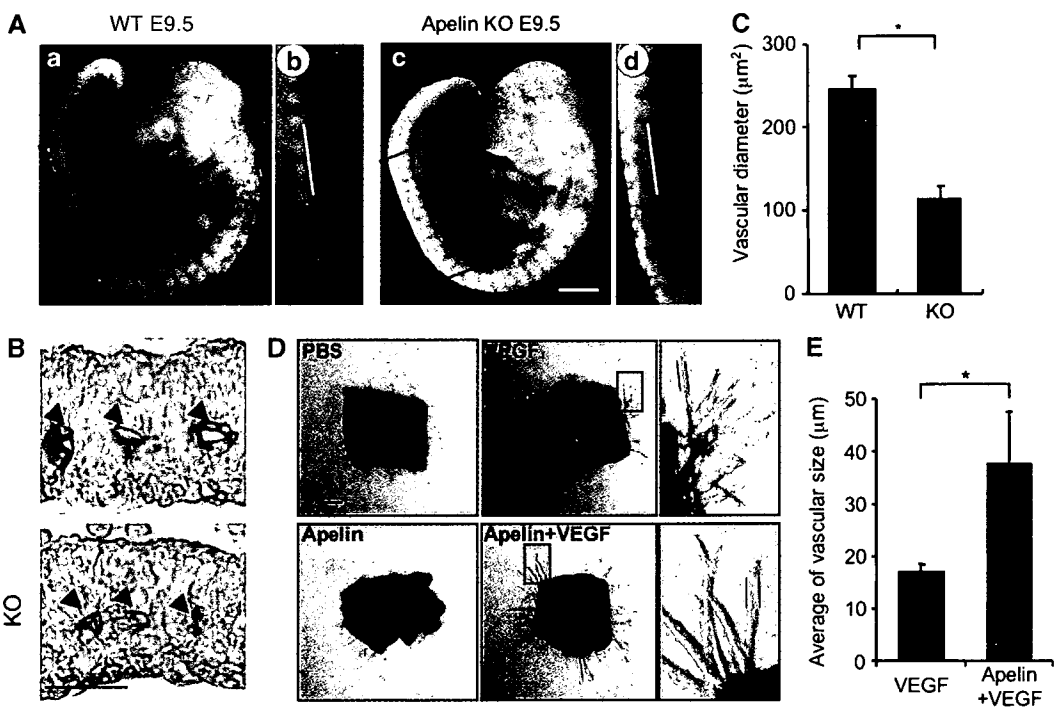

Figure 7 Defect of the enlargement in blood vessel caliber in apelin-deficient mice. (**A**) Whole-mount immunohistostaining of WT (a, b) and apelin-deficient (c, d) embryos at E9.5 with anti-CD31 Ab. (b) and (d) are higher magnifications of the areas indicated by the box in (a) and (c), respectively. Scale bar indicates 300 μm. (**B**) Sections containing ISVs (arrowheads) from WT and apelin-deficient (KO) embryos at E9.5 were stained with anti-CD31 antibody. The level of the sectioning position is indicated by a white bar in (b) and (d). Scale bar indicates 30 μm. (**C**) Quantitative evaluation of the vascular diameter of intersomitic blood vessels from apelin-deficient (KO) versus WT mice. $^*P<0.001$ (30 vessels from 5 embryos were examined). Details of the measurement of vascular diameter are shown in Supplementary Figure 7. (**D**) Representative pictures of microvessels sprouted from aortic ring using apelin-deficient mice. Aortic ring was cultured in the presence or absence of VEGF (10 ng/ml) or apelin (100 ng/ml). PBS was used as a negative control. Pictures in the right panel show a high-power view of the area indicated by the box, respectively. Scale bar indicates 300 μm. (**E**) Quantitative evaluation of the vascular size of sprouted microvessels from the aortic ring cultured as described in (D). Vascular size was measured as the length between two parallel lines as indicated in (D). $^*P<0.003$ ($n=30$).

absence of blood flow. It is known that blood flux regulates vessel size (Koller and Huang, 1999). Therefore, it is possible that shear stress may induce apelin expression in ECs. However, the results were contrary to our expectation. *In vitro* shear stress on HUVECs attenuated apelin mRNA expression in HUVECs (Supplementary Figure 13).